Polarimetric properties of X-ray pulsars

X-ray pulsars

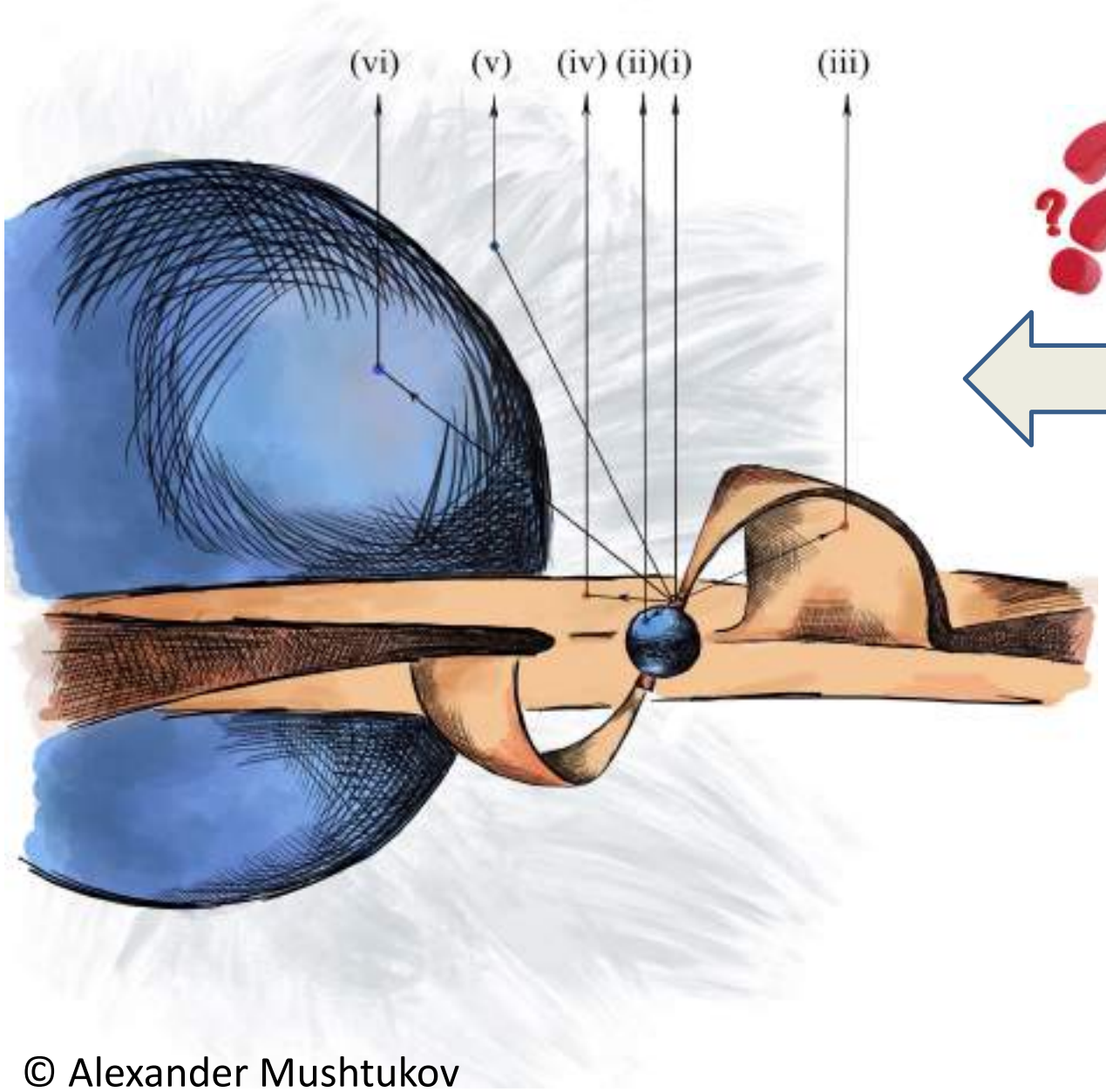

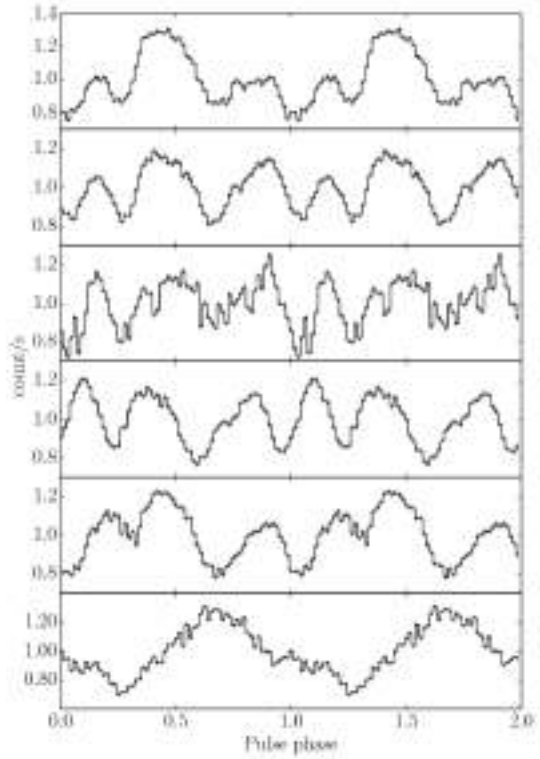

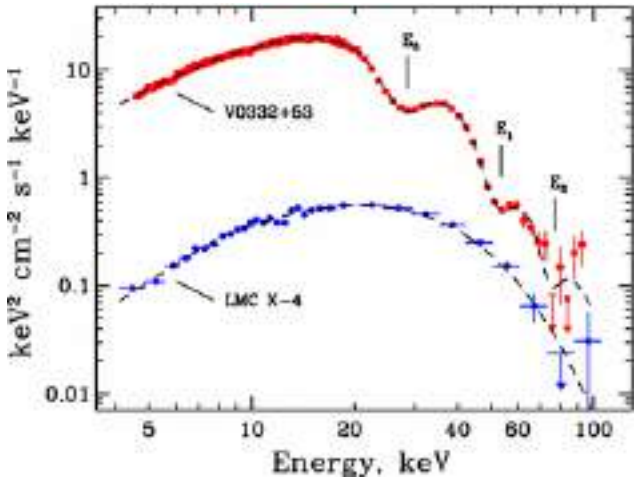

Geometry from polarimetry

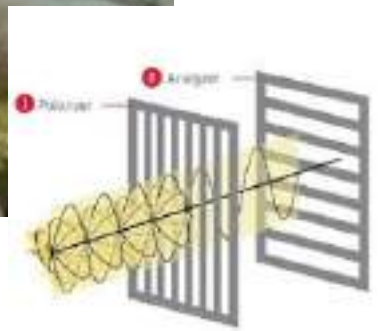

Geometry from polarimetry

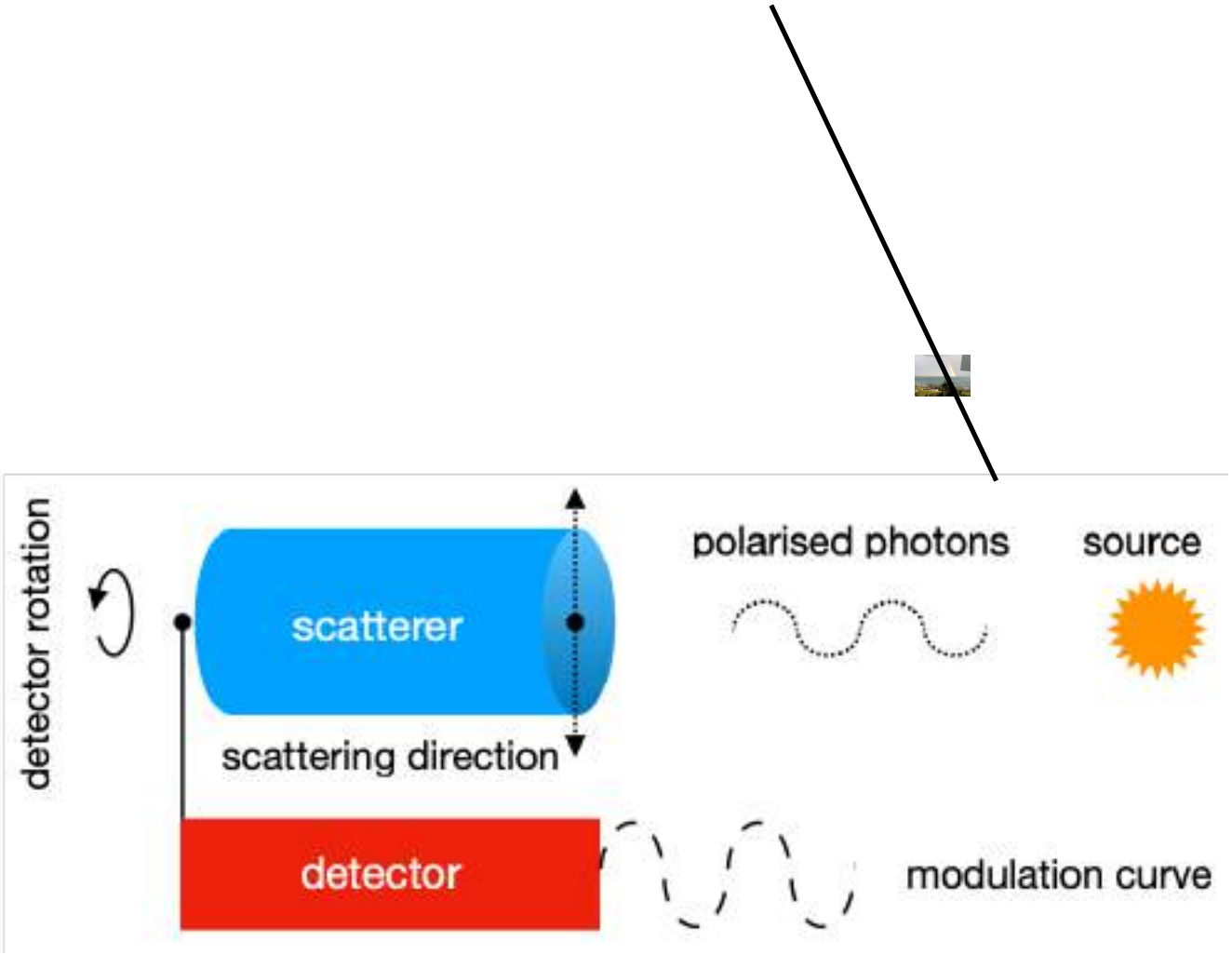

Polarimetry in X-rays

Linear polarization give us information on geometry: the degree depends on the level and kind of symmetry of the system, the angle indicates its orientation.

- First attempt to measure the X-ray polarization of the Crab Nebula back in 1969 with sounding rockets
  - PD<36% (Wolff et al. 1970)
- First X-ray nebula polarization measurement:
  PD=15.4%±5.2%, PA=156°±10° (5-20 keV)
  (Novick et al. 1972)
- New nebula polarization by OSO-8 with:
  PD=15.7%±1.5%, PA=161.1°±2.8° @2.6 keV
  PD=18.3%±4.2%, PA=155.5°±6.6° @5.2 keV
  (Weisskopf et al. 1976)
- After Pulsar subtraction (Weisskopf et al. 1978):
  PD=19.2%±1.0%, PA=156.4°±1.4° @2.6 keV
  PD=19.5%±2.8%, PA=152.6°±4.0° @5.2 keV

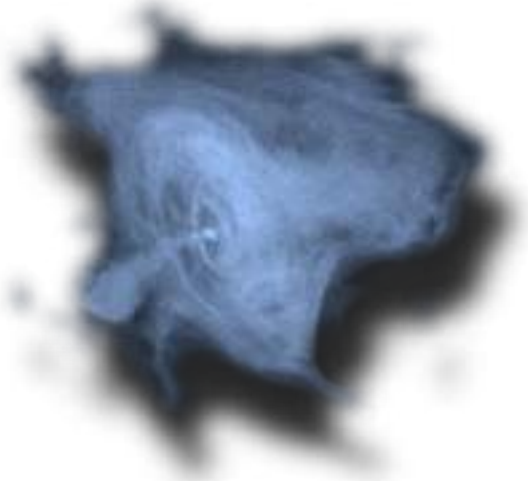

OSO-8: based on the "classical" techniques of Bragg reflection

Map of polarized X-ray sources in 2021

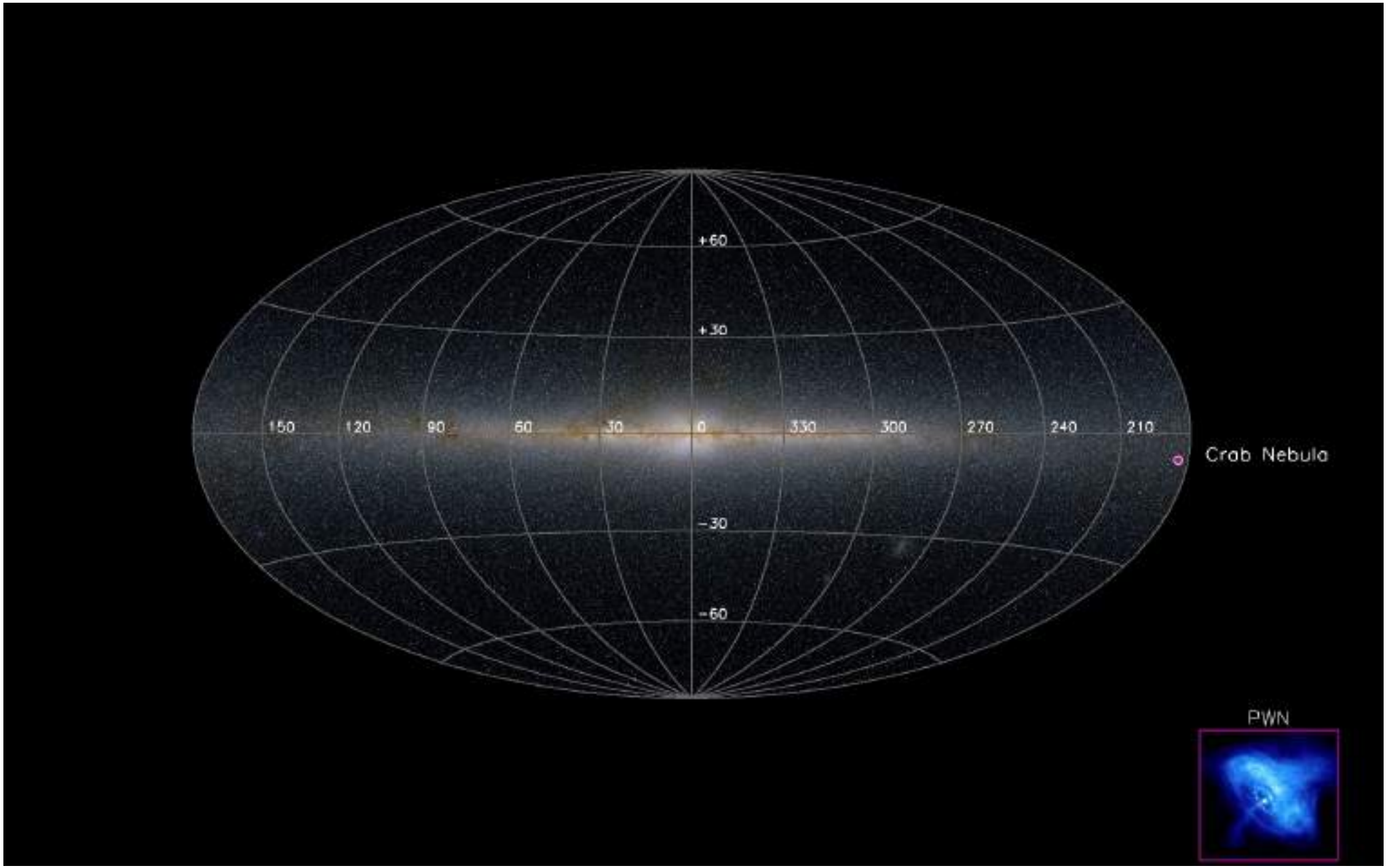

IXPE launched on 2021 Dec 9

Imaging X-ray Polarimetry Explorer

Parameter	Value
Number of mirror modules	3
Number of shells per mirror module	24
Focal length	4 m
Total shell length	600 mm
Range of shell diameters	162–272 mm
Range of shell thicknesses	0.16–0.25 mm
Shell material	Electroformed nickel–cobalt alloy
Effective area per mirror module	166 cm^2 (@ 2.3 keV); > 175 cm^2 (3–6 keV)
Angular resolution (HPD)	≤ 27 arcsec
Field of view (detector limited)	12.9 arcmin square

Three IXPE Mirror Module Assemblies

MMA, showing 24 shells

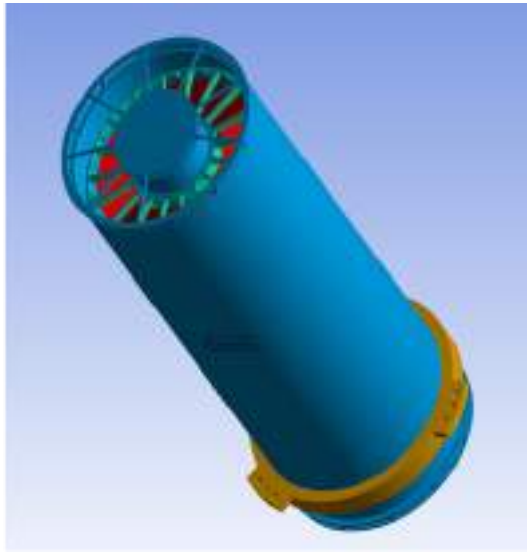

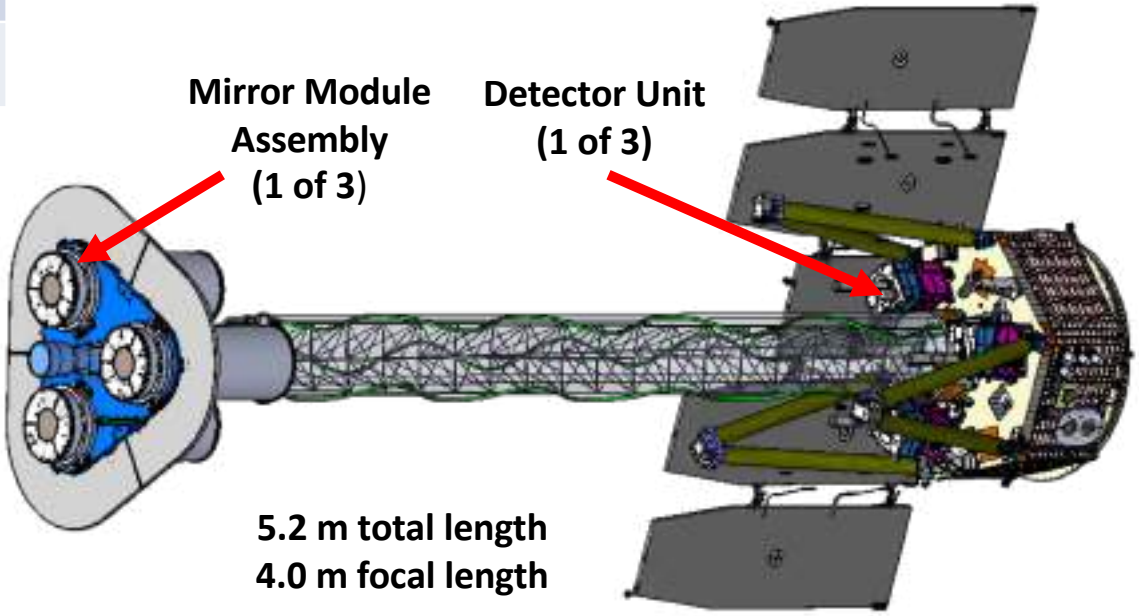

Detection Principle

- **The detection principle is based upon the photoelectric effect**

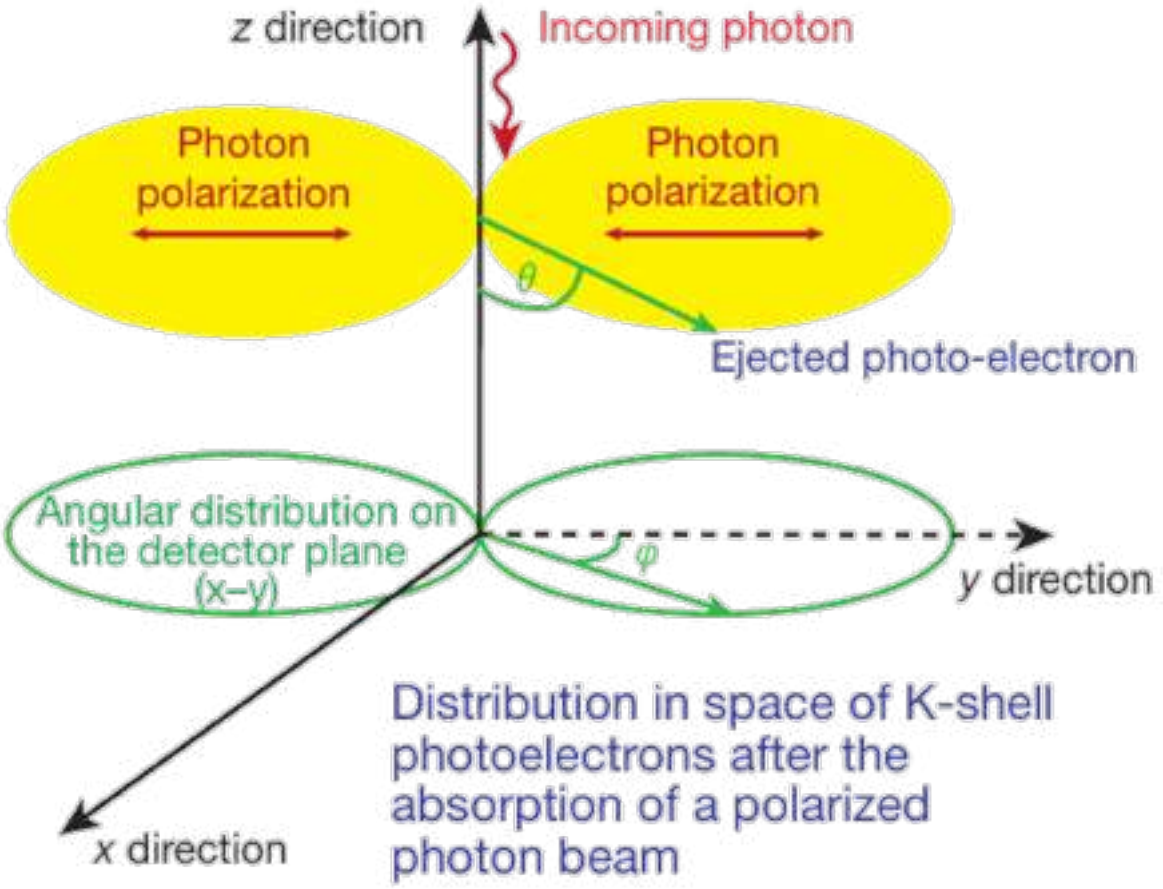

$$\frac{d\sigma}{d\Omega} = r_0^2 Z^5 \alpha_0^4 \left(\frac{1}{\beta}\right)^{7/2} 4\sqrt{2}\sin^2\theta\cos^2\varphi \ , \quad \text{where} \quad \beta \equiv \frac{E}{mc^2} = \frac{h\nu}{mc^2}$$

Gas Pixel Detector

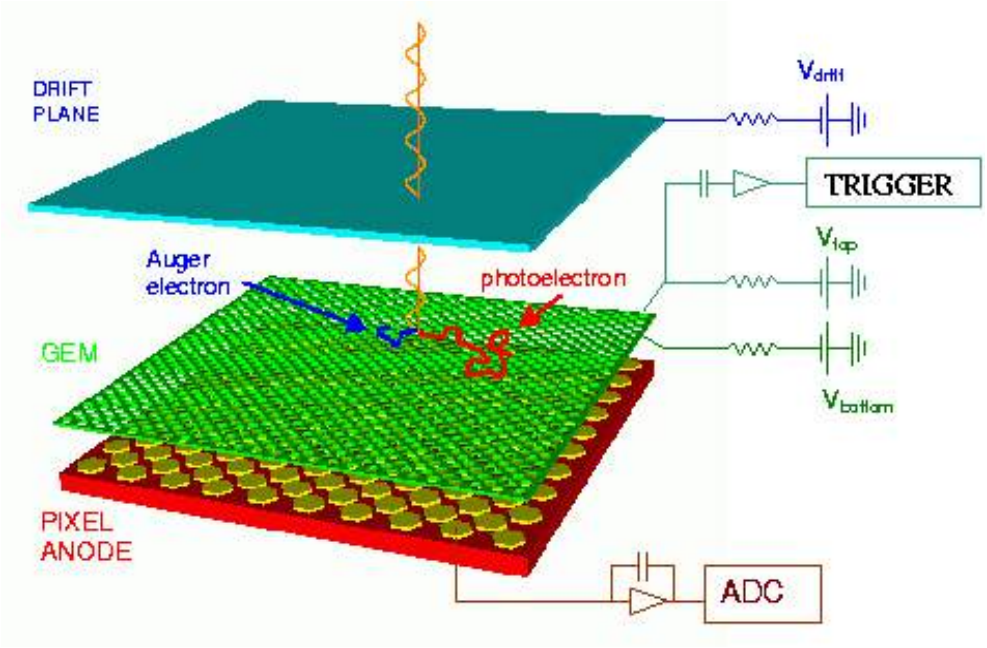

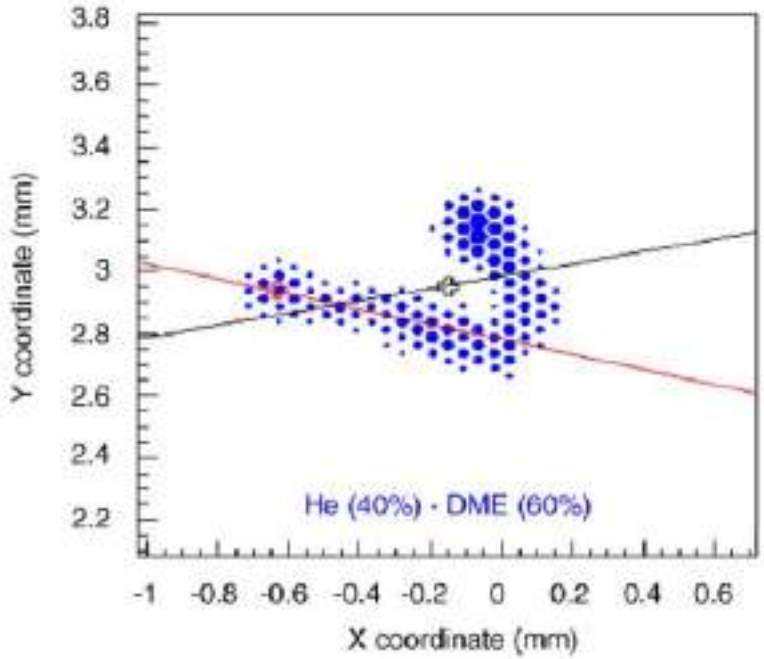

- Include a Filter & Calibration wheel with
  - Filters for specific observations (very bright sources, background)
  - Calibrations sources (polarized and unpolarized, gain)

POLARIZATION FROM MODULATION HISTOGRAM AND CALIBRATED MODULATION FACTOR

- **Polarization degree**
  - $\Pi = \text{Modulation}/\mu(E)$

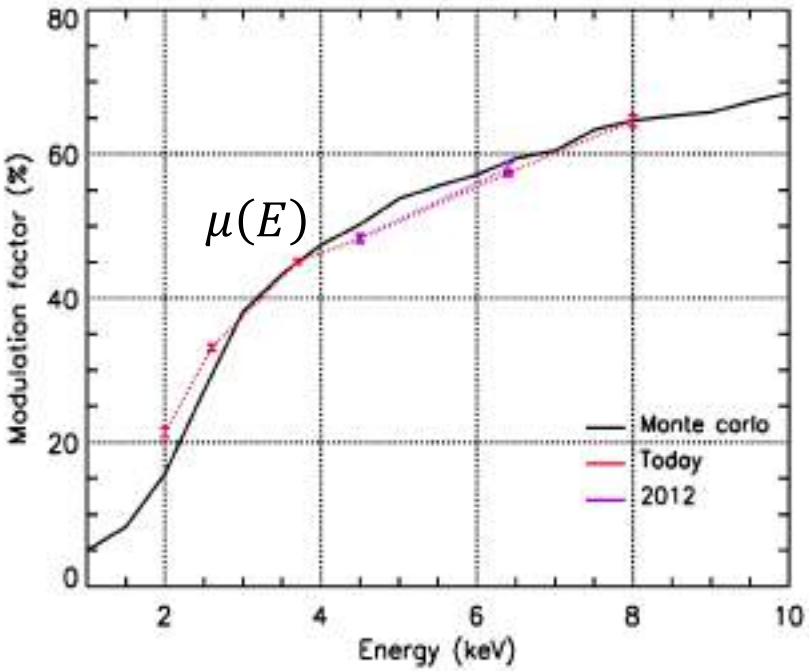

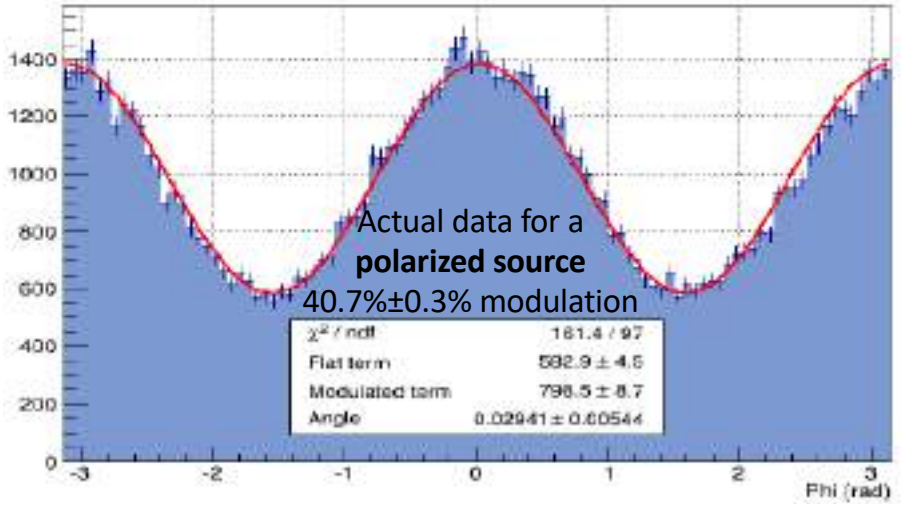

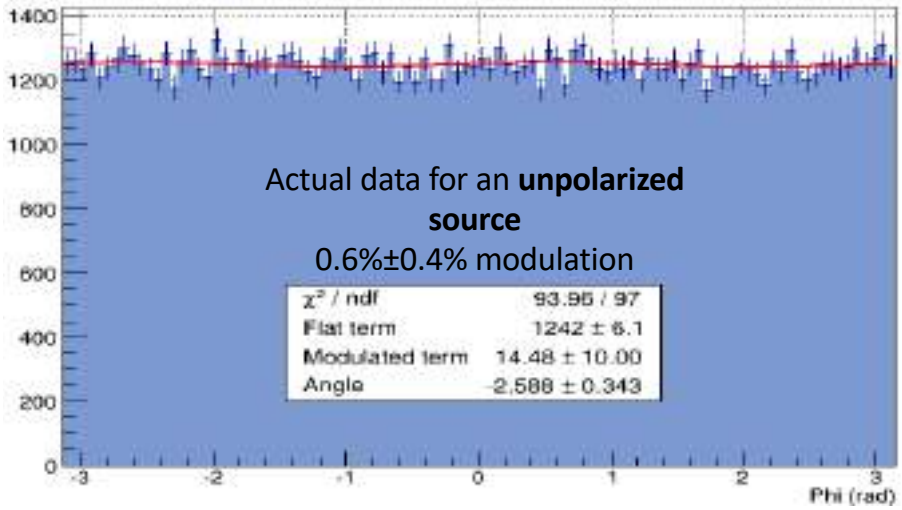

SKY MAP OF X-RAY POLARIZED SOURCES IN 202(5?)

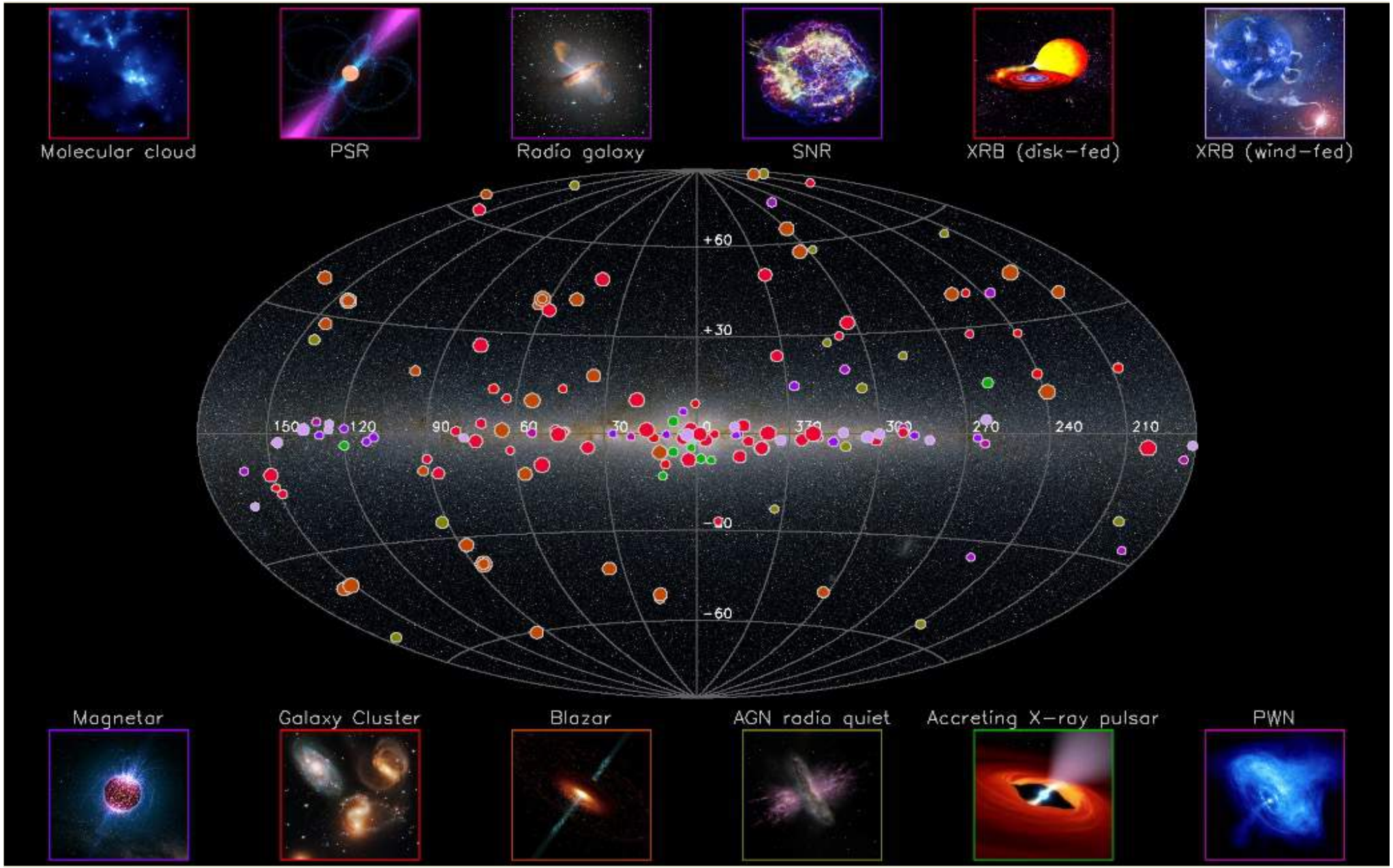

Polarization properties of X-ray pulsars

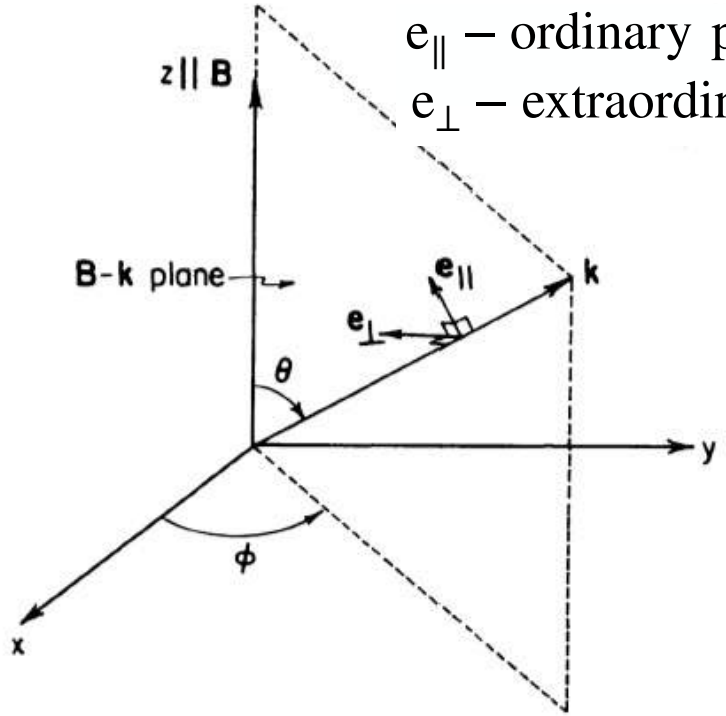

$e_{||}$ – ordinary photons

$e_{\perp}$ – extraordinary photons

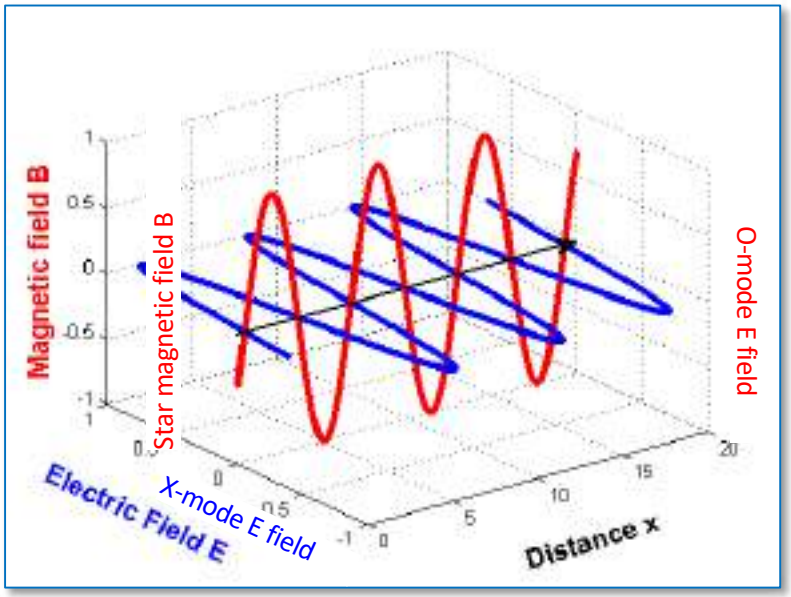

O-mode: the **E**-field oscillates in the **k-B** plane

X-mode: the **E**-field oscillates ⊥ to the **k-B** plane

The opacity of the X-mode is drastically reduced compared to that of the opacity of the O-mode. Consequently, the emergent radiation is dominated by the X-mode, which comes from the deeper and hotter layers of plasma, and so is strongly polarized in the direction of the X-mode.

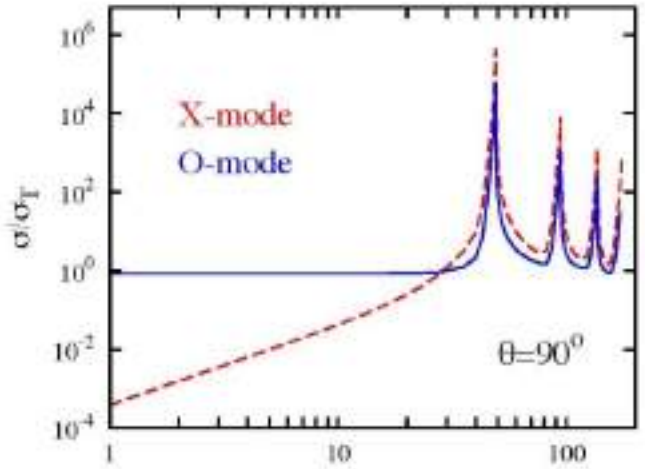

Mushtukov et al. 2016

Polarization properties of X-ray pulsars

Beam pattern of the emerging radiation is determined by the geometry of the emission region. Two main configurations of the emission regions can be distinguished depending on the local mass accretion rate.

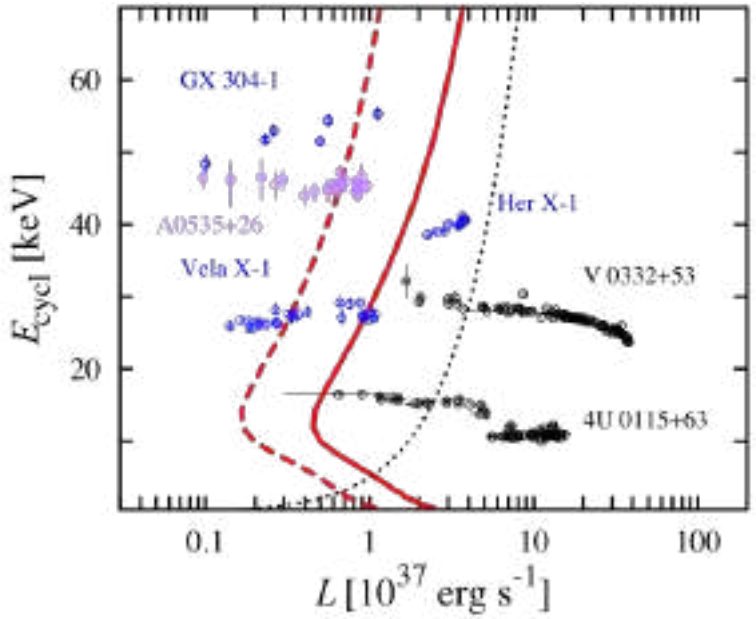

The critical luminosity L* separating these two regimes of accretion is a function of physical and geometrical parameters of the system and for typical XRP is estimated to be about 10^{37} erg/s (Basko & Sunyaev 1975; Becker et al. 2012; Mushtukov et al. 2015).

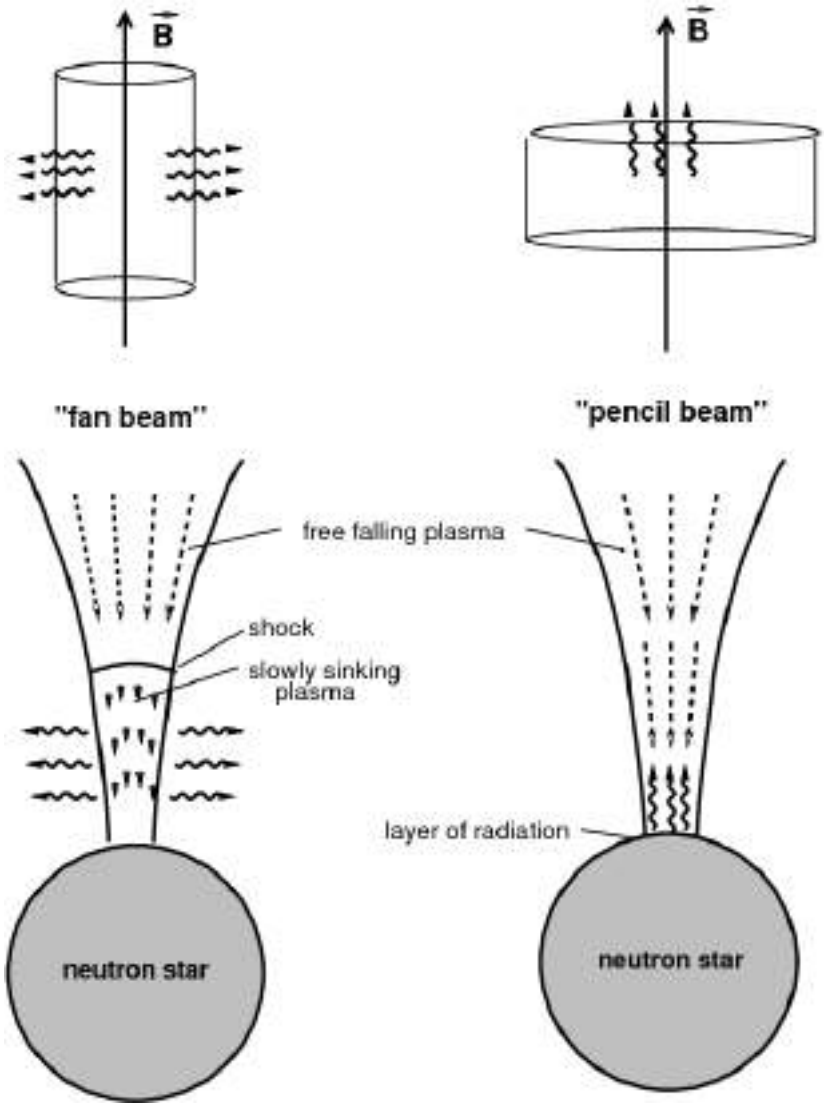

Polarization properties of X-ray pulsars

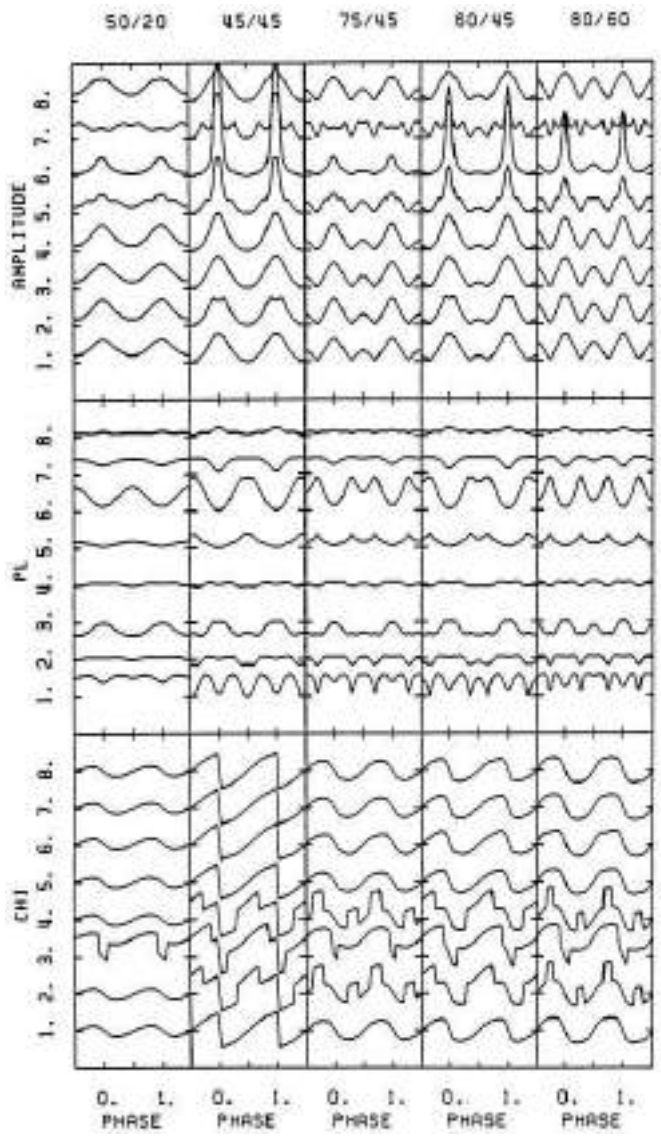

Pencil beam

Fan beam

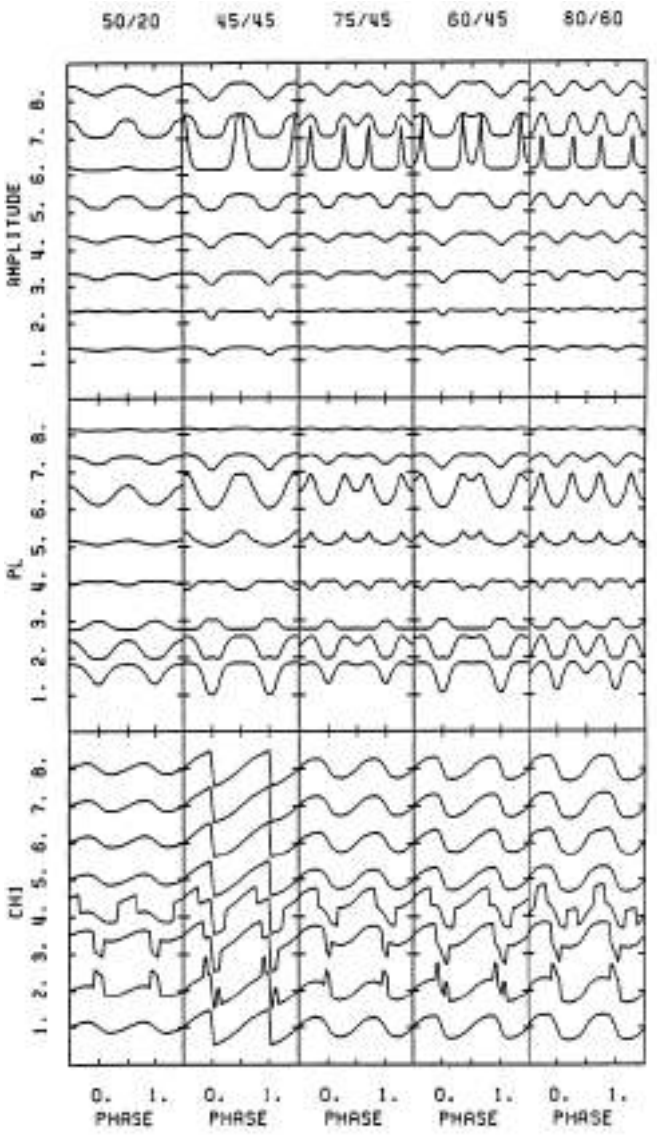

Meszaros et al. 1988

Polarization properties of X-ray pulsars

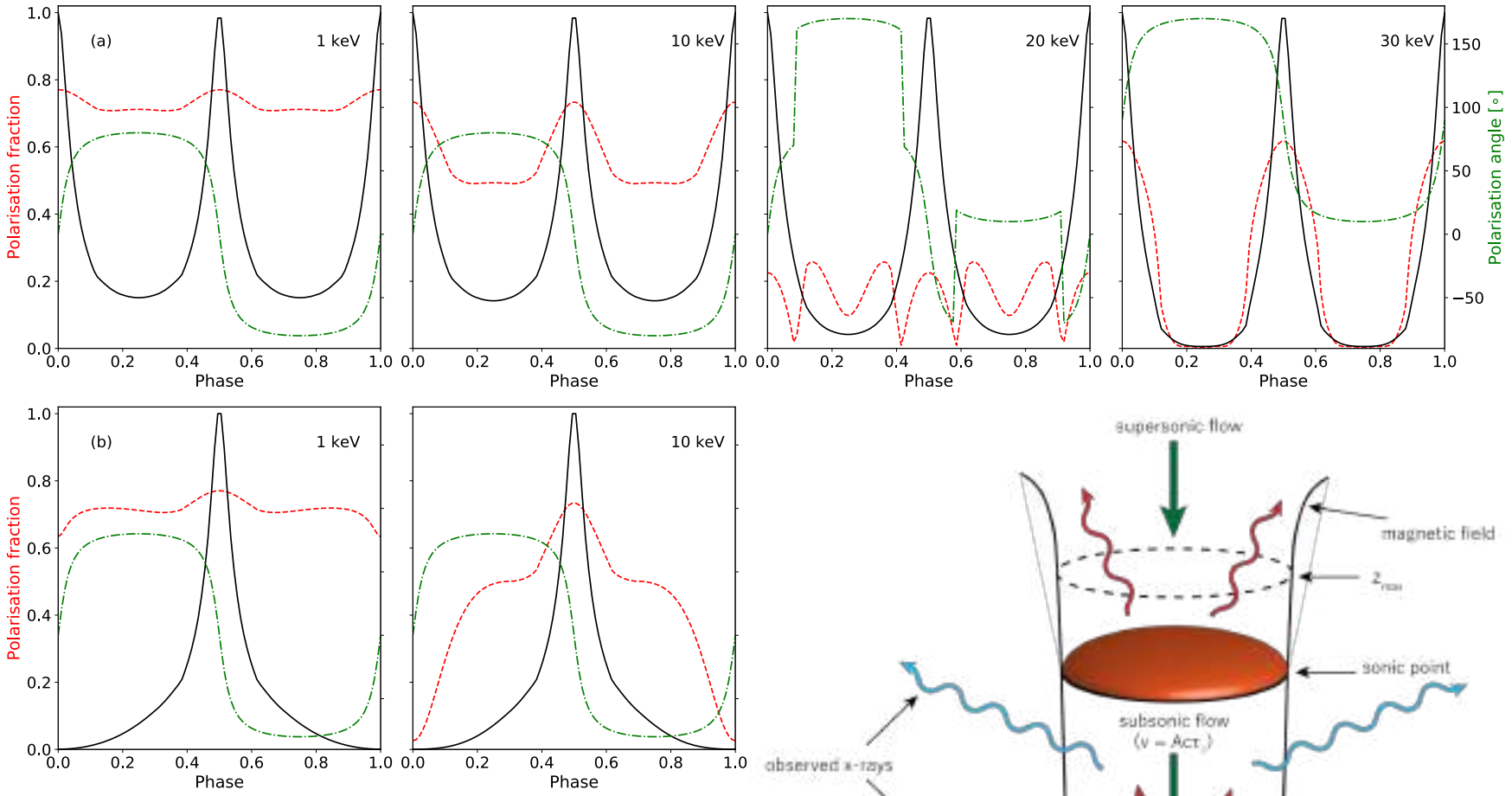

Figure 15. Polarisation parameters as a function of phase and energy for four different models: (a) two-column, $z_{max} = 6.6$ km, (b) one-column, $z_{max} = 6.6$ km,

Caiazzo & Heyl, 2021

X-ray pulsars observed by IXPE

Cen X-3 (ApJ Letters)
Her X-1 (Nature Astronomy)
4U 1626-67 (ApJ)
Vela X-1 (ApJ Letters)
GRO J1008-57 (A&A)
EXO 2030+375 (A&A)
X Per (MNRAS)
GX 301-2 (A&A)
More Her X-1 (Nature Astronomy)
LS V +44 17/RX J0440.9+4431 (A&A)
Swift J0243.6+6124 (A&A)
SMC X-1 (A&A)

Pulse phase-resolved polarimetry: Cen X-3

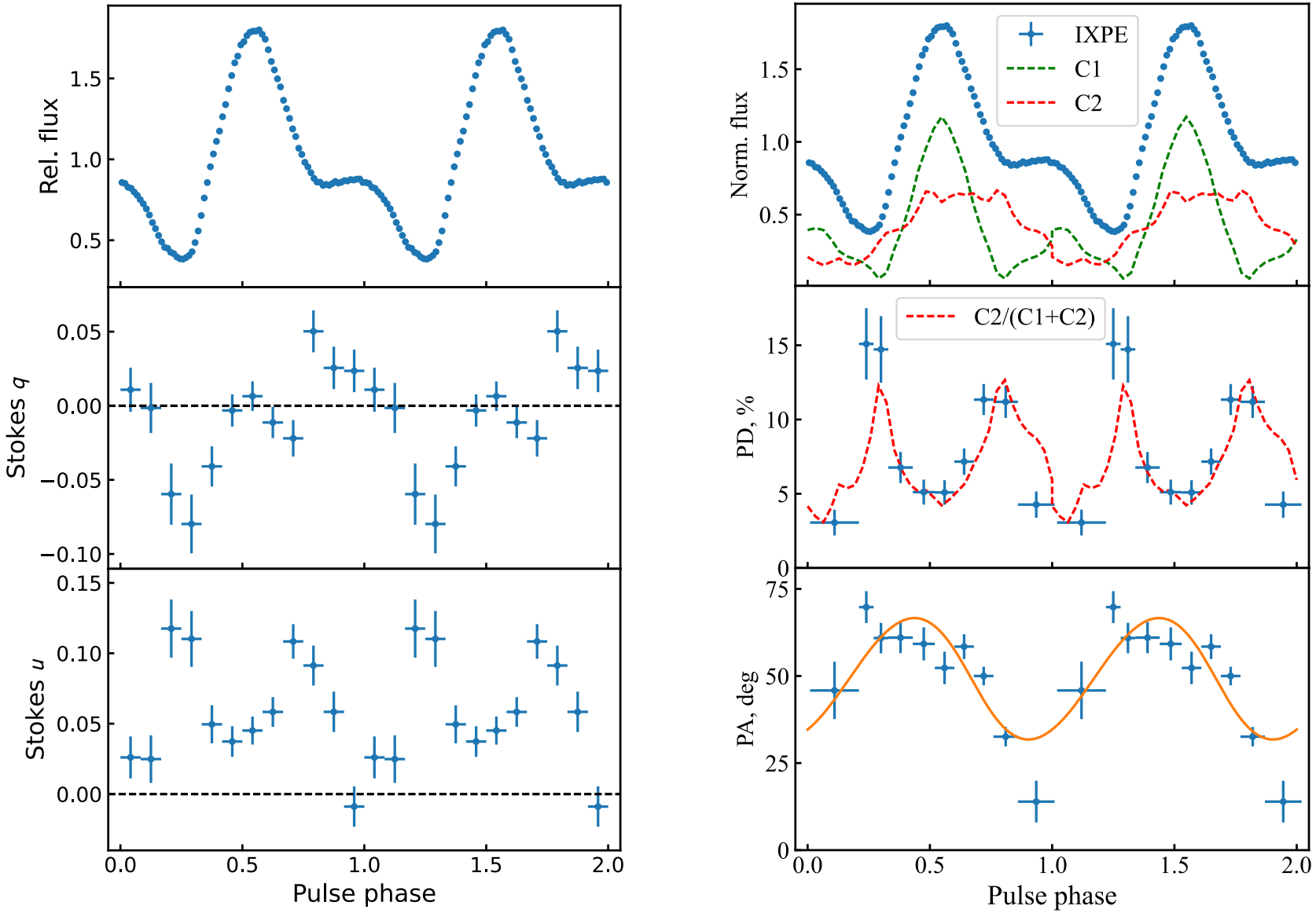

Tsygankov+, 2022, ApJL

Low polarization degree

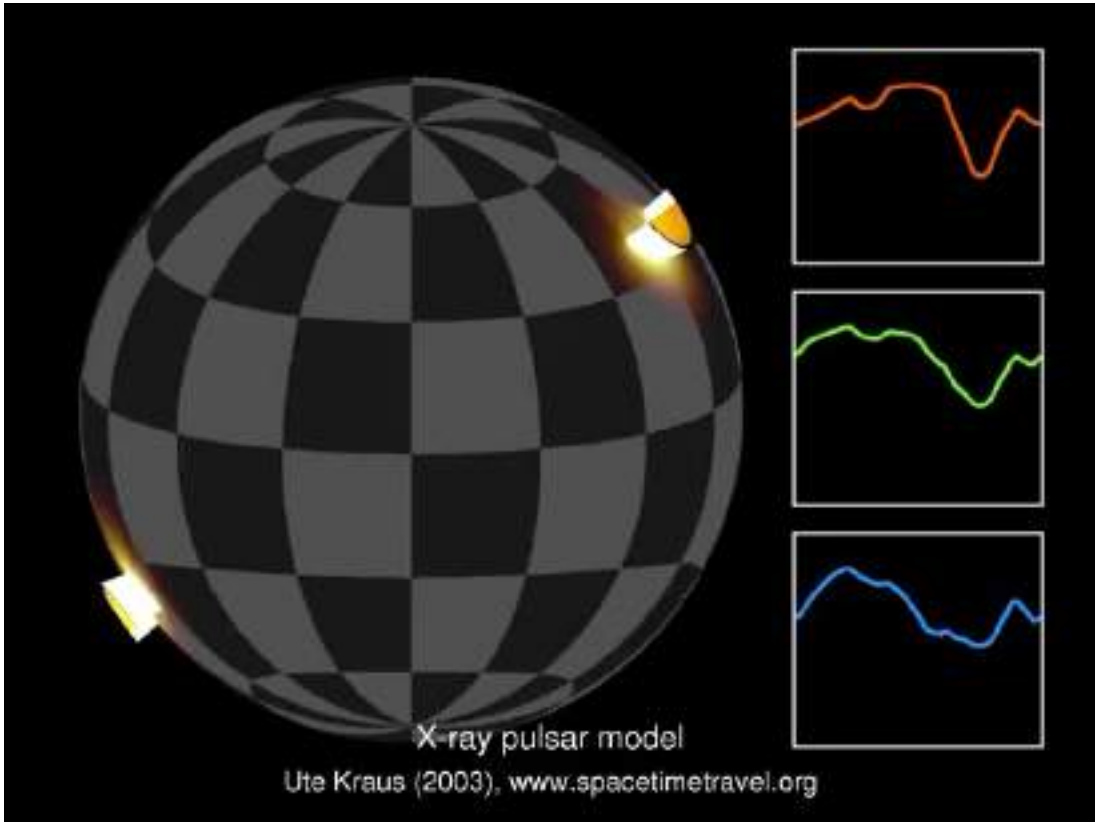

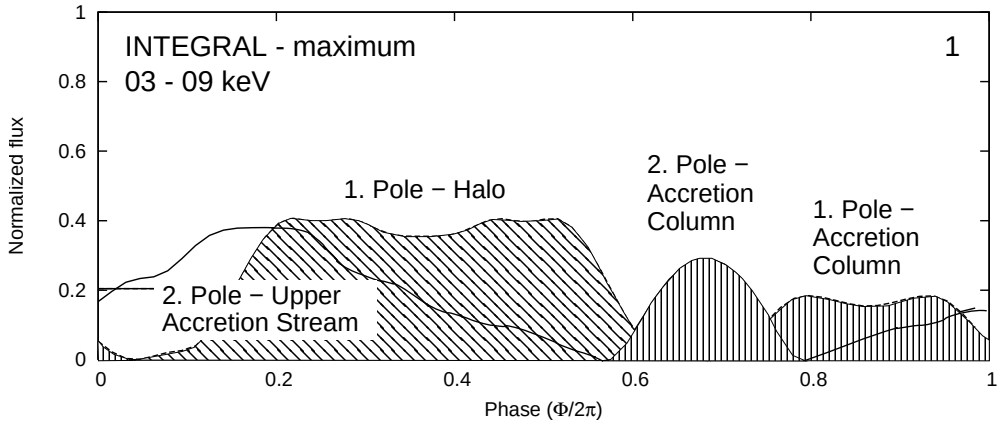

Kraus 96, 2003, Sasaki et al, 2012

Geometry of the system

Rotating vector model

$$\tan(\mathrm{PA} - \chi_\mathrm{p}) = \frac{-\sin\theta\ \sin(\phi - \phi_0)}{\sin i_\mathrm{p}\ \cos\theta - \cos i_\mathrm{p}\ \sin\theta\ \cos(\phi - \phi_0)}$$

Poutanen 2020

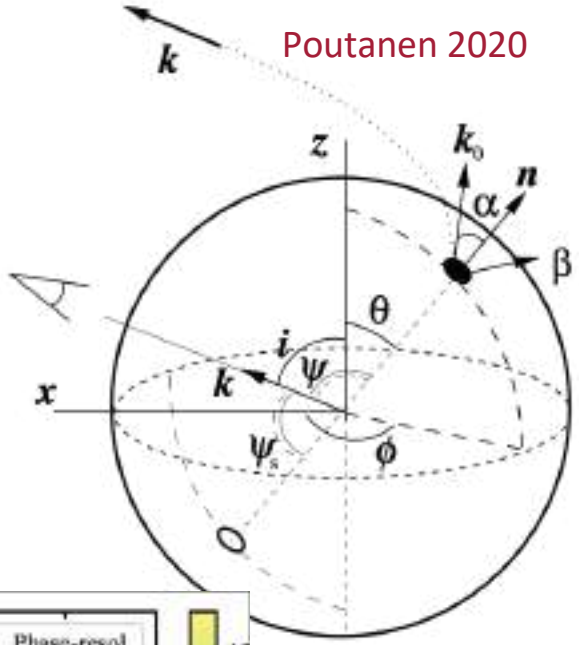

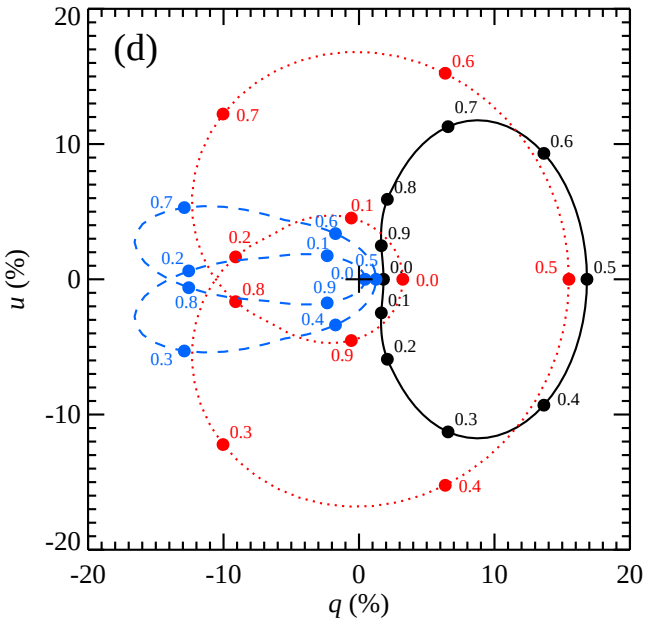

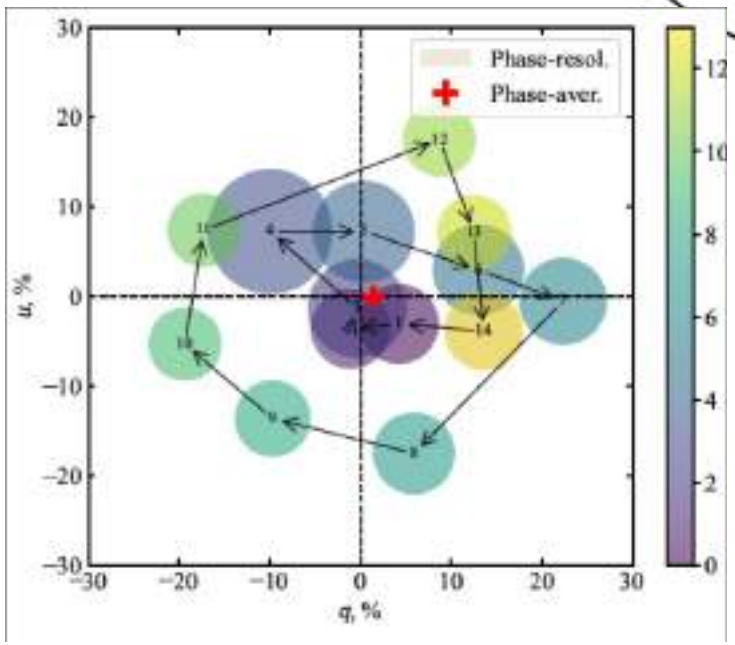

Rotating vector model -> geometry

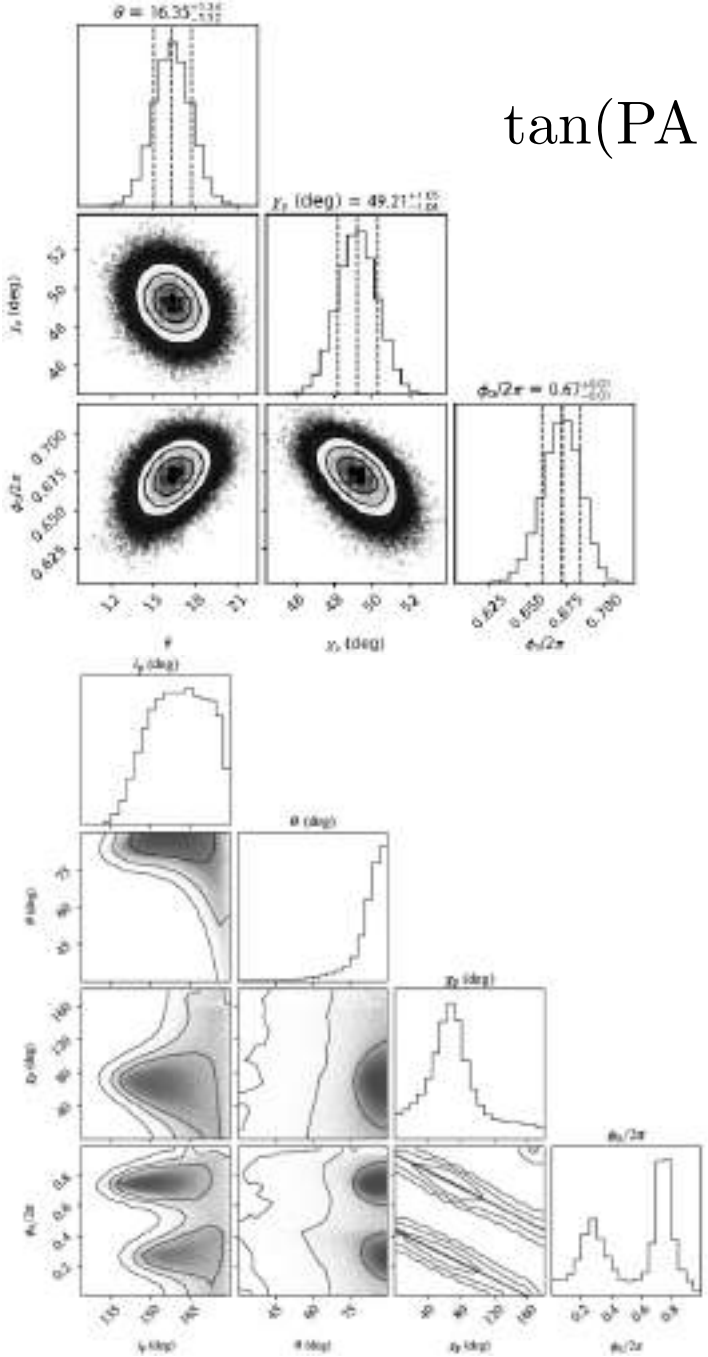

$$\tan(\mathrm{PA} - \chi_\mathrm{p}) = \frac{-\sin\theta \;\; \sin(\phi - \phi_0)}{\sin i_\mathrm{p} \cos\theta - \cos i_\mathrm{p} \sin\theta \cos(\phi - \phi_0)}$$

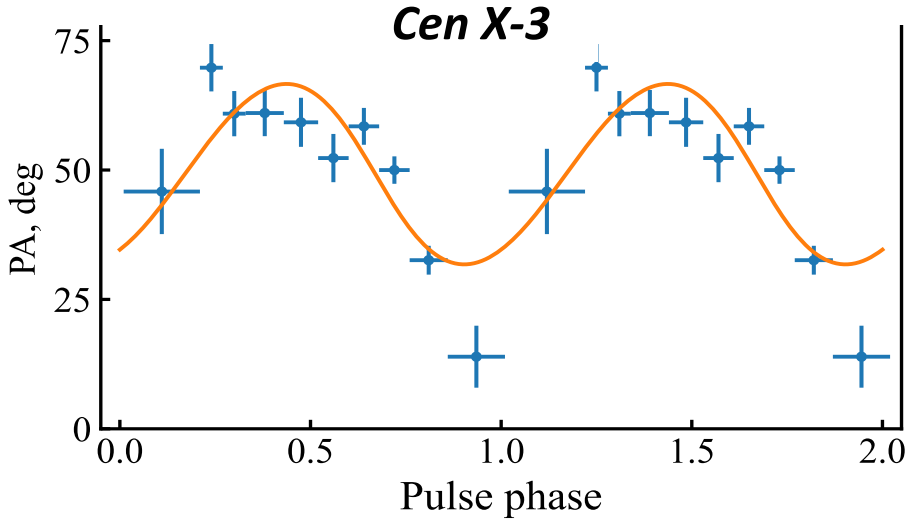

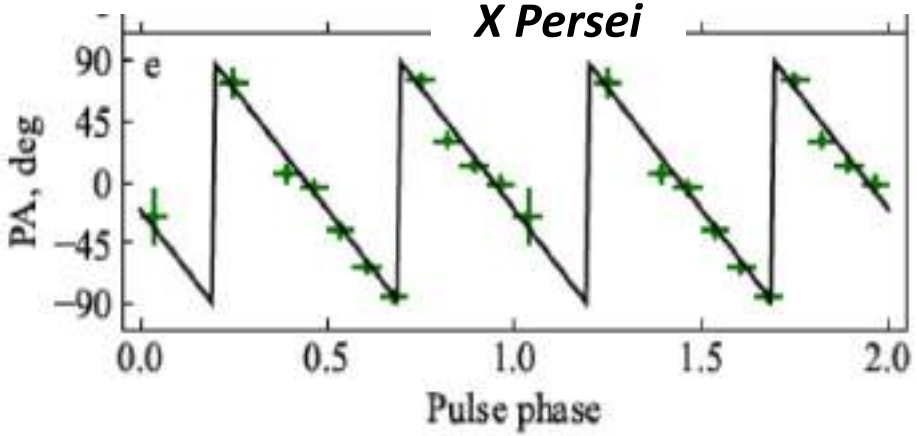

Tsygankov+, 2022, ApJL
Mushtukov+, 2023, MNRAS

IXPE observations of Her X-1

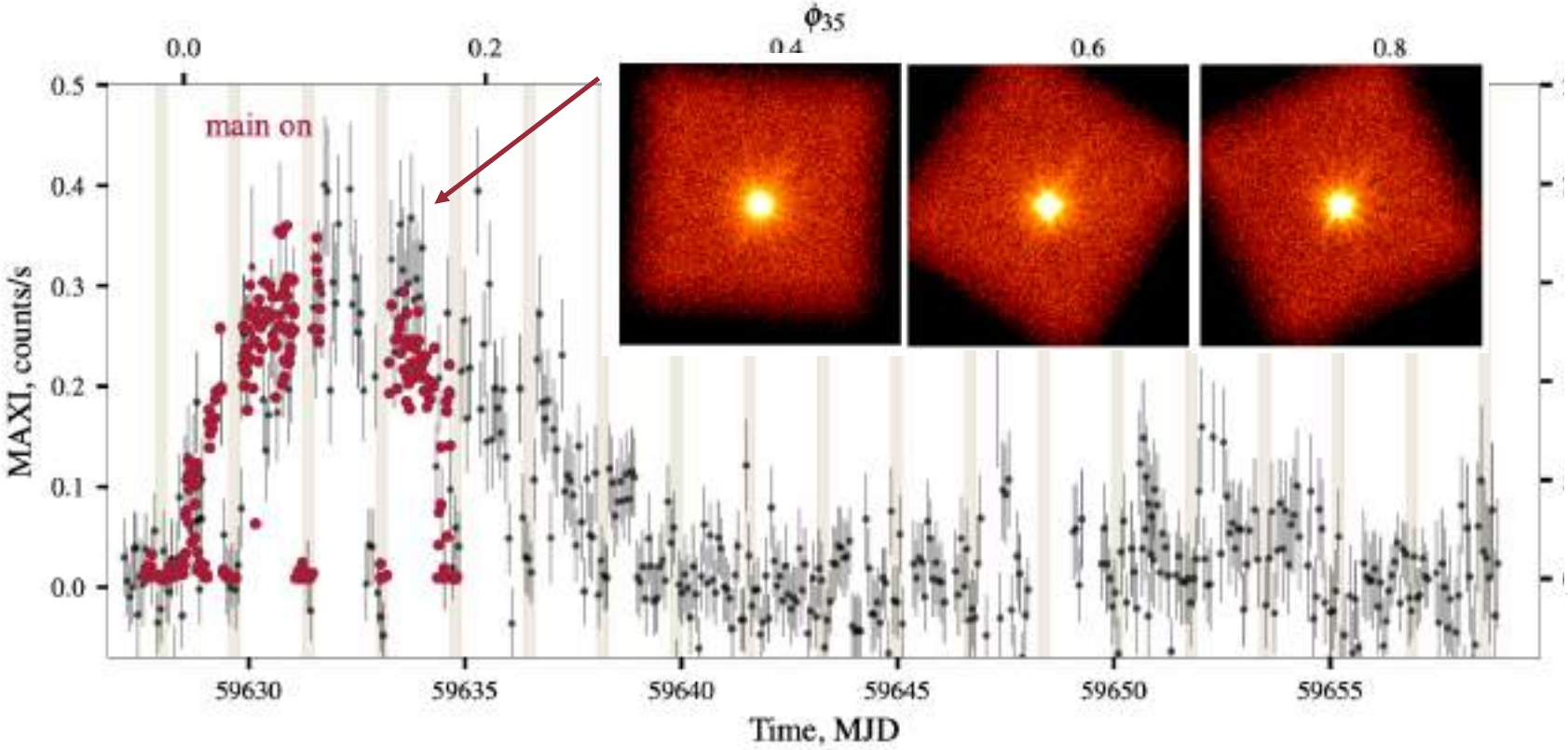

- Spin period: 1.24 s
- Orbital period: 1.7 d
- Super-orbital period: 35 d

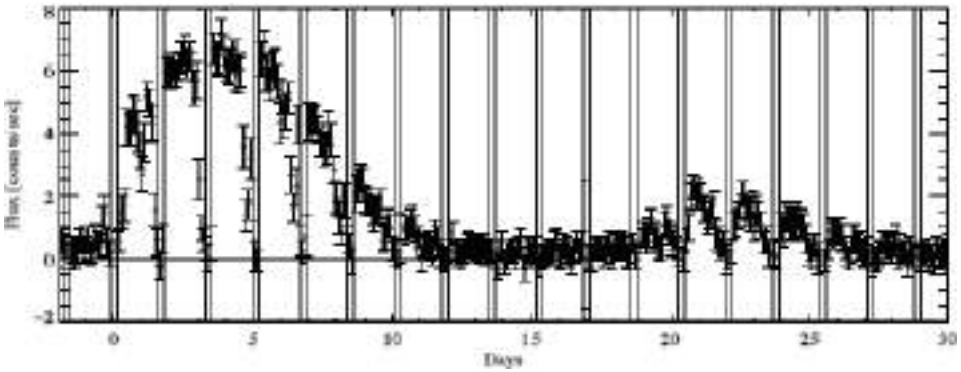

Doroshenko+, 2022, NatAst

Time dependence of X-ray polarization

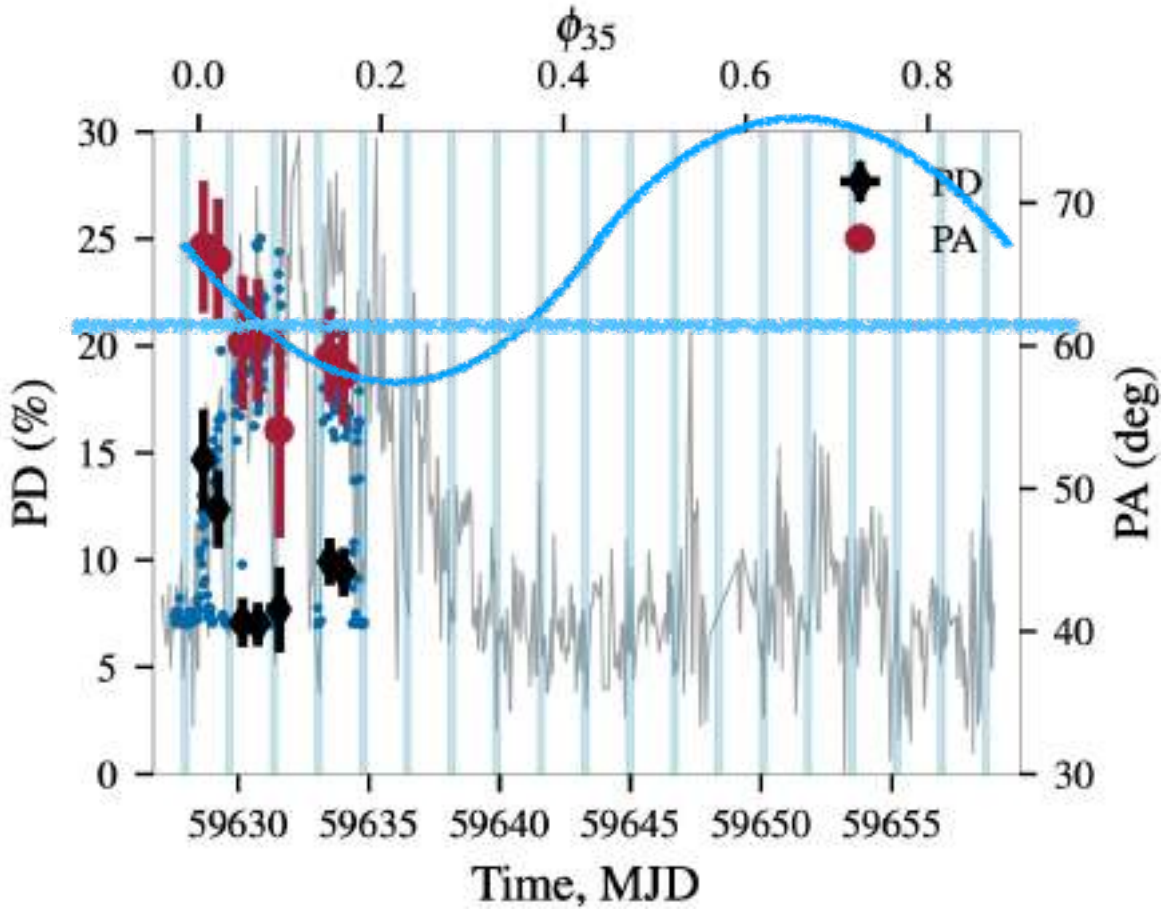

- Variability of both PD/PA with time (not very significant)
- More observations during the short-on are needed to check if average PA or amplitude of its variations change.

Second observation of Her X-1

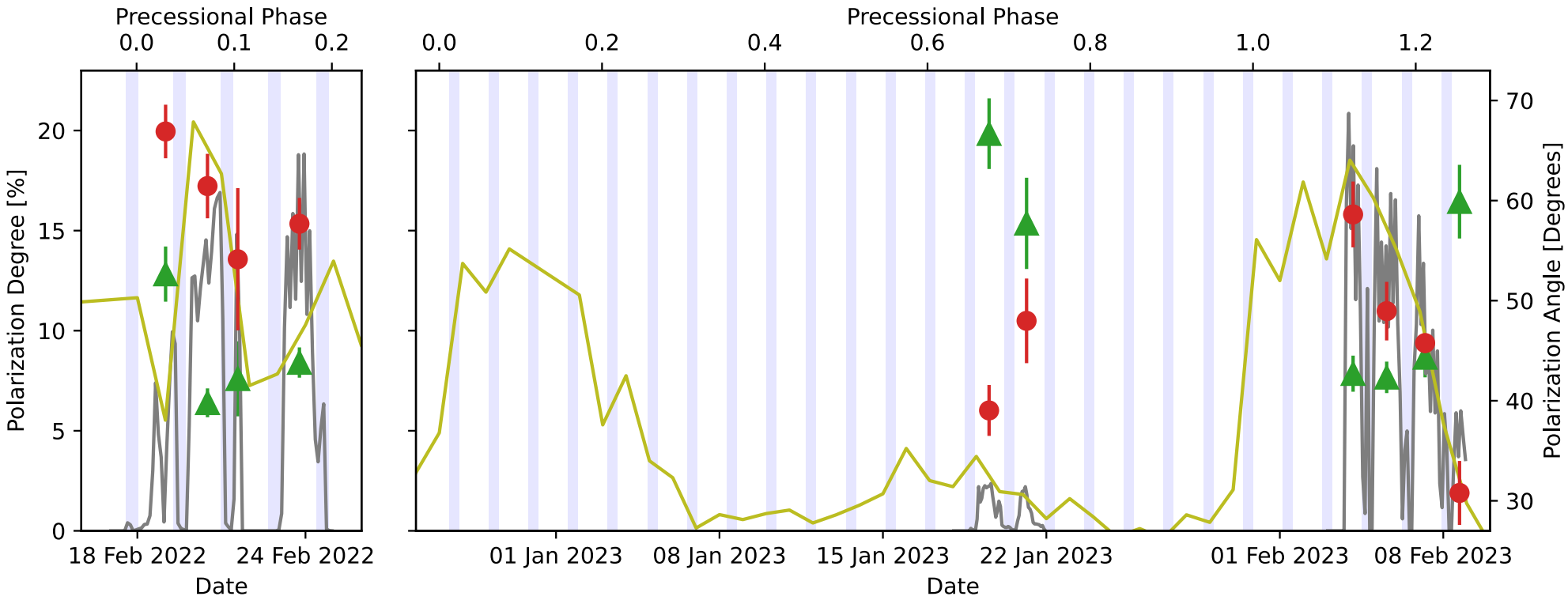

Heyl+, NatAst, 2024.

Second observation of Her X-1

	Mean PD (%)	$i_{\rm p}$ (deg)	θ (deg)	$\chi_{\rm p}$ (deg)	ϕ_0 (%)	Prec. Phase (%)
First Main-On	9.5 ± 0.5	58^{+28}_{-22}	$14.5^{+3.0}_{-4.0}$	55.4 ± 1.6	$19.0^{+2.7}_{-2.2}$	8.8
Early	8.6 ± 0.6	64^{+25}_{-22}	$16.3^{+3.5}_{-4.1}$	57.9 ± 2.1	$19.0^{+2.6}_{-2.4}$	7.3
Late	9.3 ± 0.7	85^{+35}_{-37}	$15.9^{+3.6}_{-4.0}$	52.2 ± 2.7	$21.7^{+4.5}_{-5.0}$	16.2
Short-On	17.8 ± 1.4	90^{+30}_{-30}	$3.7^{+2.6}_{-1.9}$	41.9 ± 2.2	85.1^{+18}_{-19}	68.7
Second Main-On	9.1 ± 0.5	56^{+24}_{-20}	$16.0^{+3.1}_{-4.3}$	46.8 ± 1.5	$19.8^{+2.3}_{-2.0}$	15.9

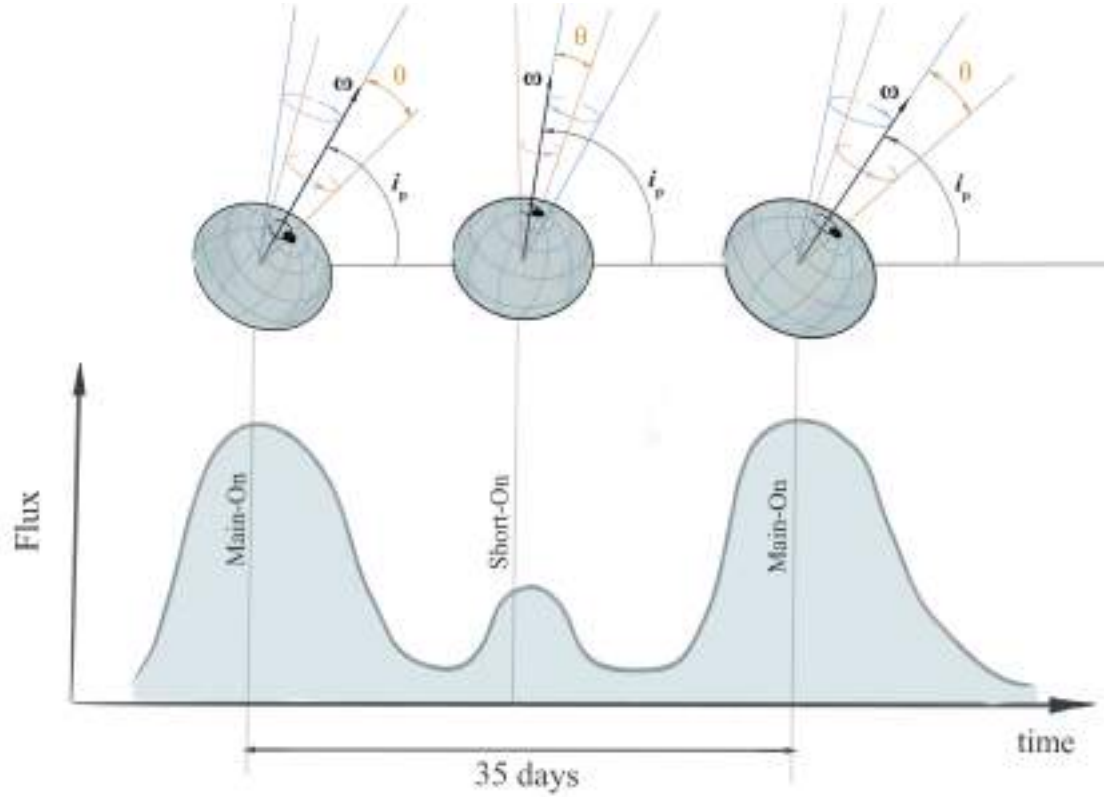

Heyl+, NatAst, 2024.

IXPE observations of LS V +44 17/RX J0440.9+4431

Active for the first time since 2010-11, onset of a Giant (Type II) outburst in Jan 2023

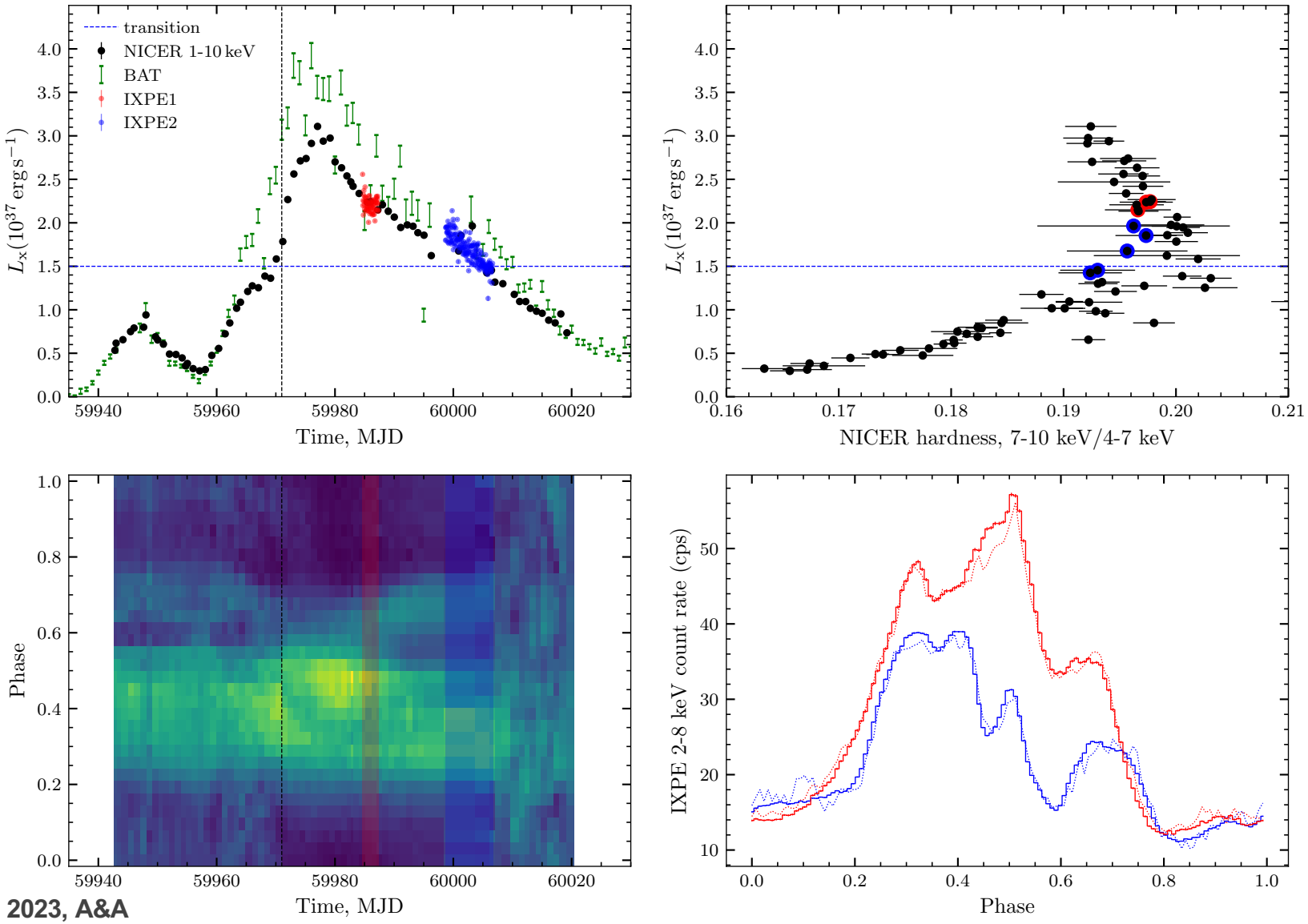

Doroshenko+, 2023, A&A

IXPE observations of LS V +44 17/RX J0440.9+4431

RVM:

$$\tan(\chi-\chi_p)=\frac{-\sin\delta\,\sin[2\pi(\phi-\phi_0)]}{\sin i_p\cos\theta-\cos i_p\sin\theta\cos[2\pi(\phi-\phi_0)]}$$

Exquisite statistics, yet like other XRPs both observations consistent with the Rotating Vector model (RVM, Radhakrishnan&Cooke 1969)

PCUBEs results consistent with simplified (power-law/CompTT) spectro-polarimetry

Geometry is dramatically different. The angles changed by

$$\Delta i_p \sim 46^\circ$$
$$\Delta\theta_p \sim 30^\circ$$
$$\Delta\chi_p \sim 90^\circ$$
$$\Delta\phi_0 \sim 0.5$$

...in 10 days

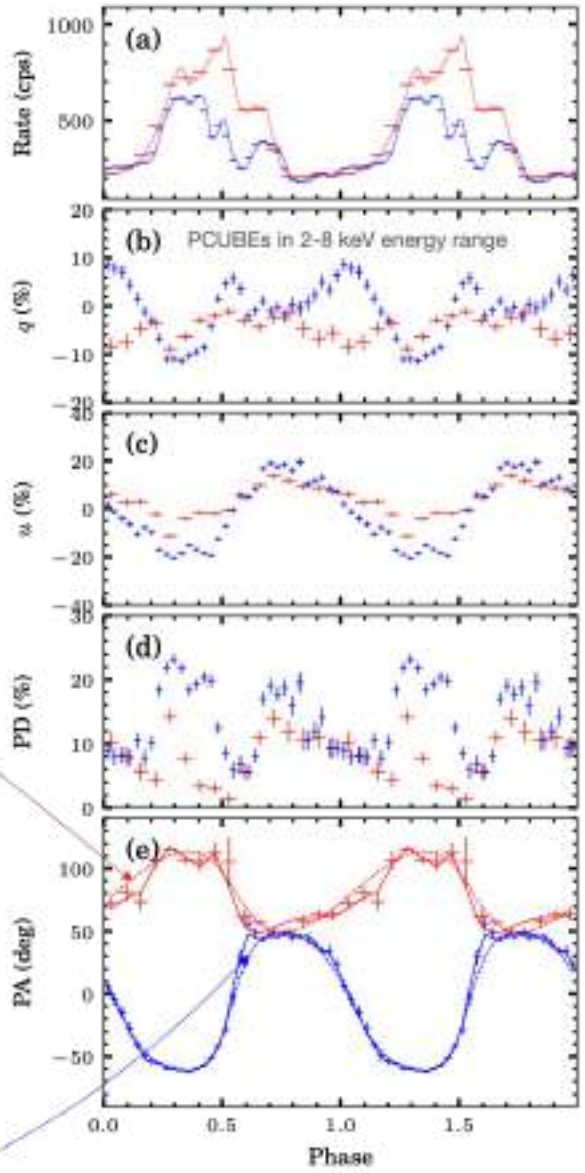

Doroshenko+, 2023, A&A

IXPE observations of LS V +44 17/RX J0440.9+4431

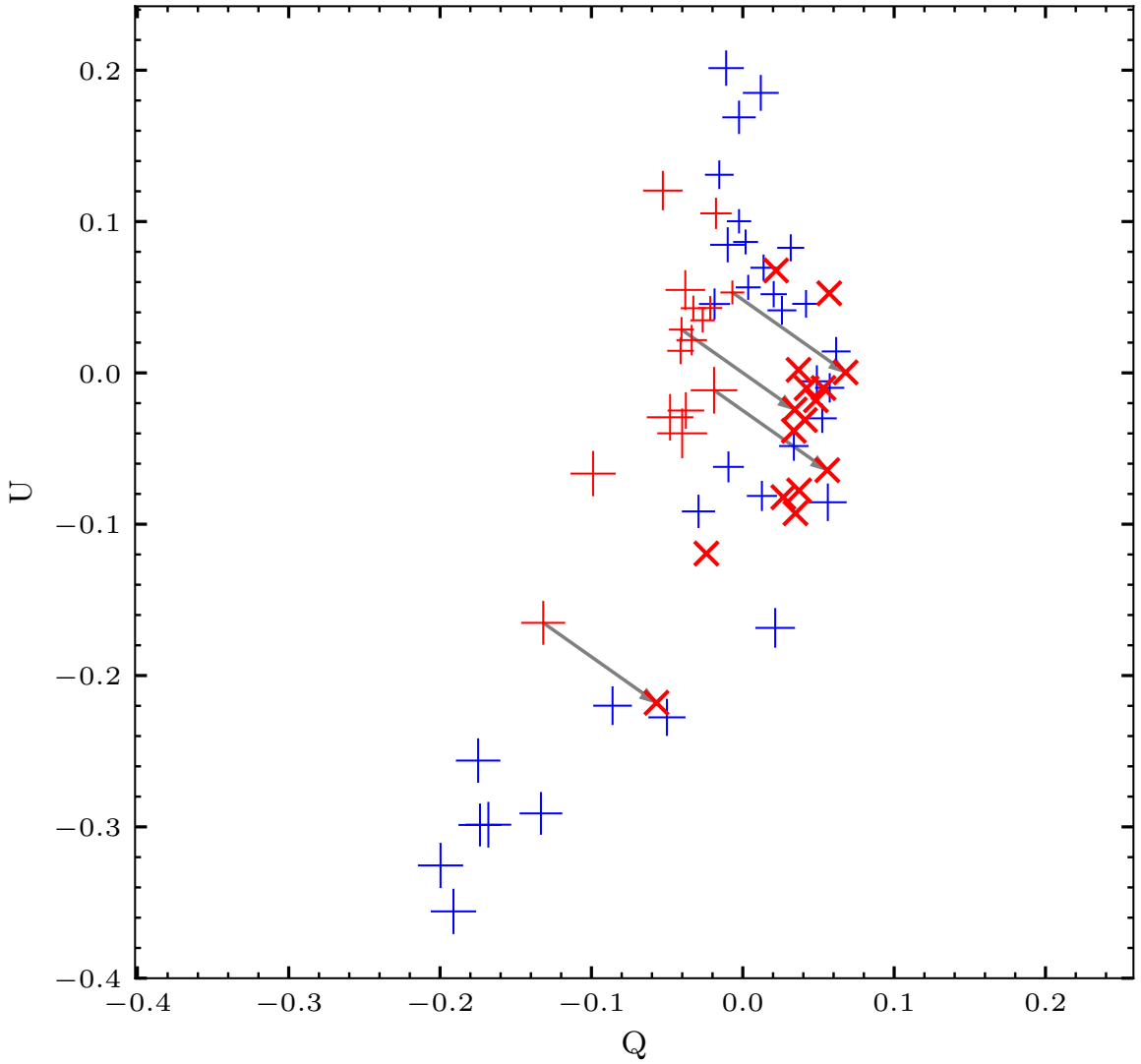

There appears to be a constant shift in Q/U space between the two observations, i.e. additional constant polarised component? Re-define the model…

IXPE observations of LS V +44 17/RX J0440.9+4431

Work in Q/U space

$$
\begin{aligned}
I(\phi) &= I_0 + I_1(\phi), \\
Q(\phi) &= Q_0 + P_1(\phi) I_1(\phi) \cos[2\chi(\phi)], \\
U(\phi) &= U_0 + P_1(\phi) I_1(\phi) \sin[2\chi(\phi)].
\end{aligned}
$$

observed constant RVM-part

$$
\tan(\chi - \chi_p) = \frac{-\sin\theta \, \sin[2\pi(\phi - \phi_0)]}{\sin i_p \cos\theta - \cos i_p \sin\theta \cos[2\pi(\phi - \phi_0)]}
$$

- Assume constant + RVM components
- RVM parameters constrained through comparison with observed Q/U
- **Only $I_{0,1} \times P_{0,1}$ is constrained, not flux P individually** *(can have low-intensity strongly polarised background or high-intensity weakly polarised background)*
- Some limits can be obtained based on conditions $I_0 < I_{1,min}$, $P_0 < 1$, $P_1 < 1$, $P_0 > P_0(I_0/I_{min})$

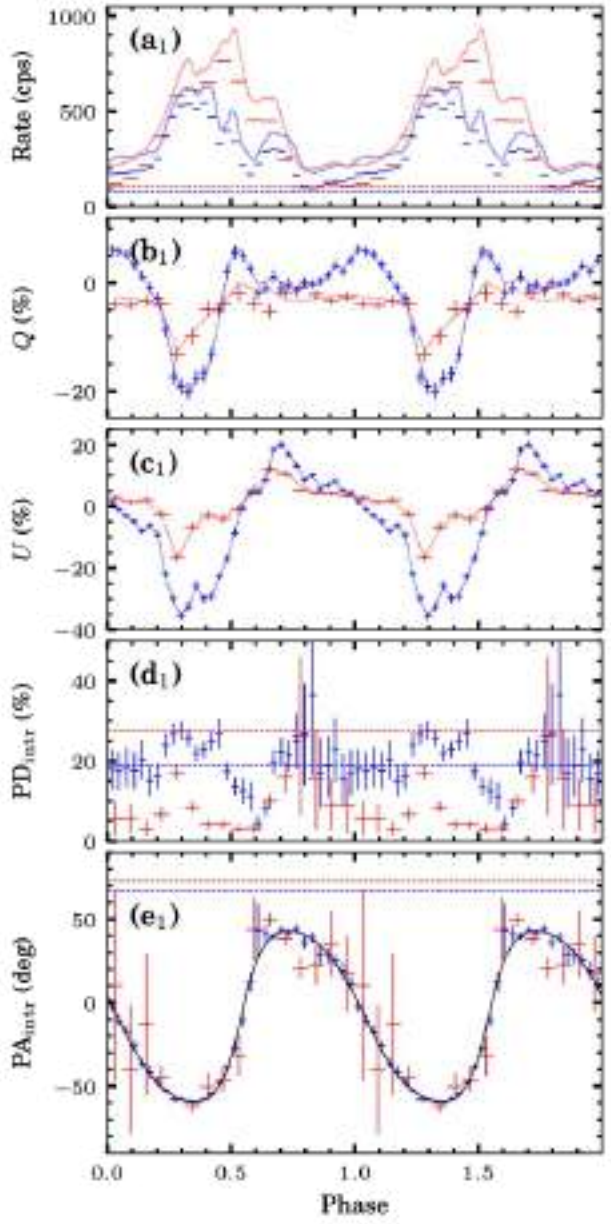

(after subtracting constant component)

Doroshenko+, 2023, A&A

IXPE observations of LS V +44 17/RX J0440.9+4431

- **Three questions:**
  - what is it?
  - can it give 10-40% of observed flux?
  - 30% polarisation?
- **Unpulsed = relatively far away from NS: scattering in disk/disk wind?**
  - **PD up to ~33%** due to comptonization in accretion disk atmosphere (Sunyaev&Titarchuk 1985) or outflows
    - **~20% polarization** observed in Cyg X-3/Circinus (scattering)
  - There's evidence for presence of strong disk outflows in BeXRBs from radio and X-ray data (Jaisawal et al. 2019; Doroshenko et al 2020, van den Eijnden et al. 2019, 2022; Chatzis et al. 2022; van den Eijnden et al. 2022) with **up to 20% flux in reflected/scattered component** (although at higher L_x).
  - LS V +4417 is viewed **~edge-on**, polarization due to scattering is expected to be high (i.e. fraction of scattered emission may remain low)

Geometries of different XRPs

Her X-1

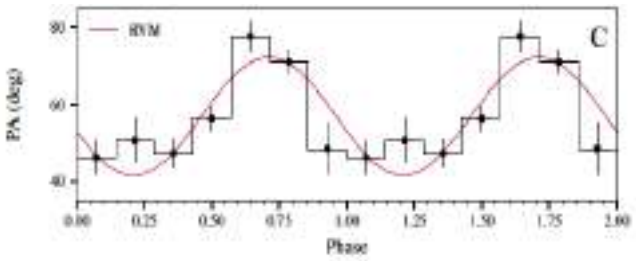

Cen X-3

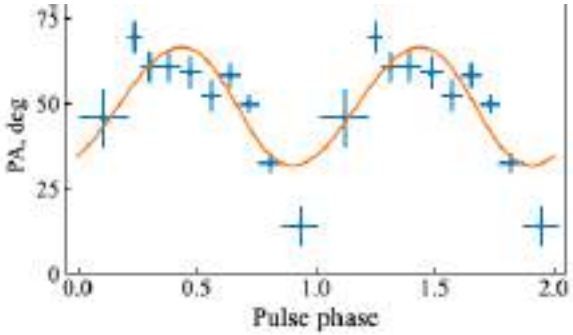

X Persei

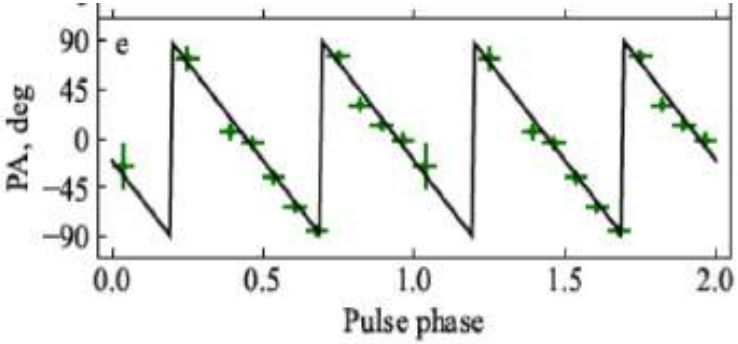

GX 301-2

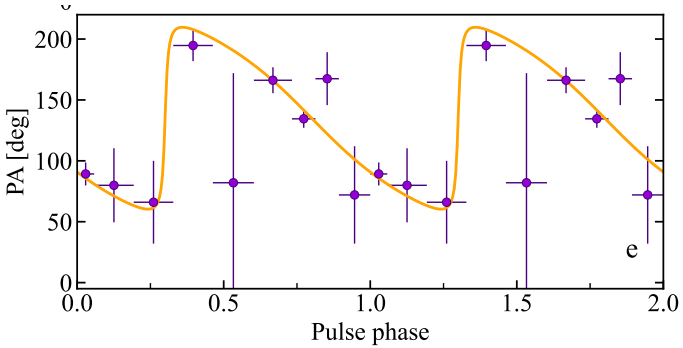

GRO J1008-57

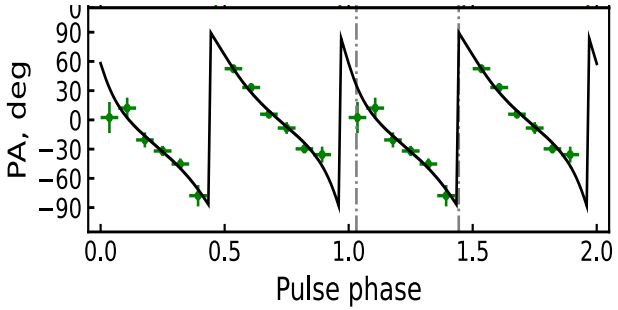

EXO 2030+375

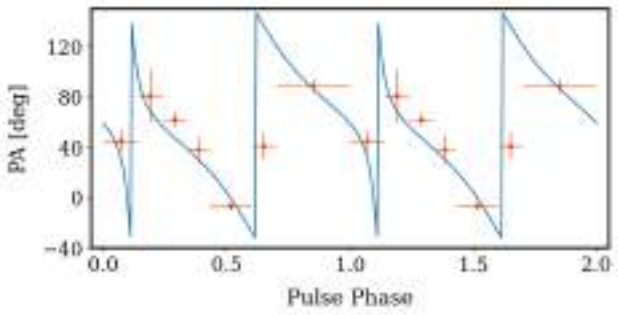

Geometries of different XRPs

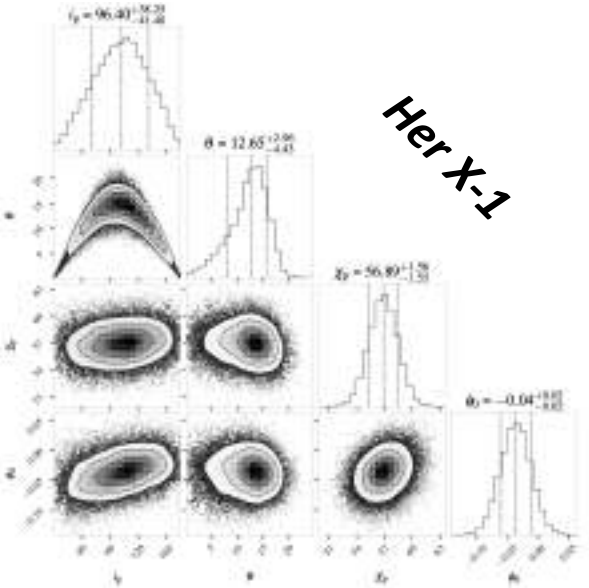

Her X-1

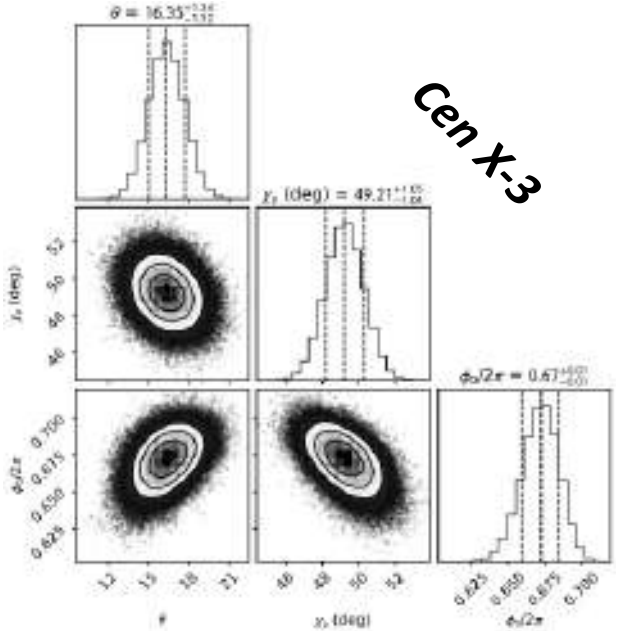

Cen X-3

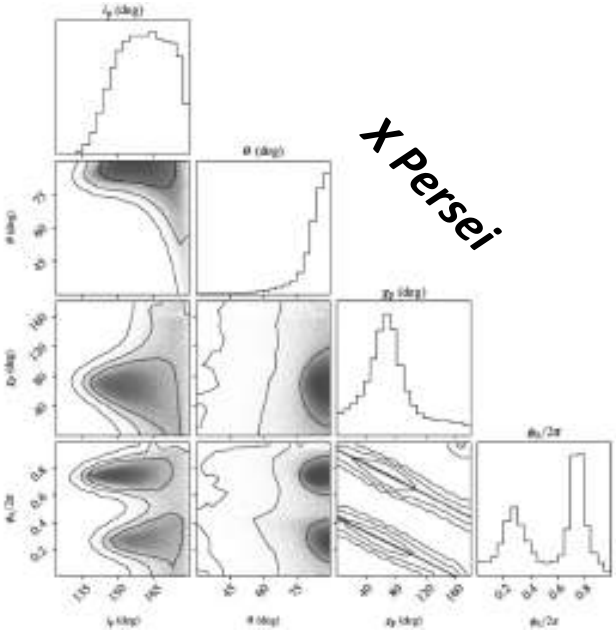

X Persei

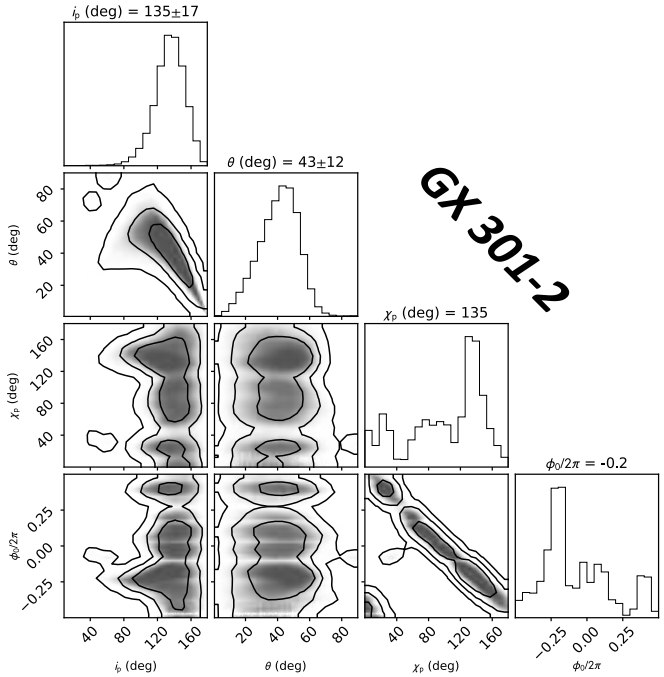

GX 301-2

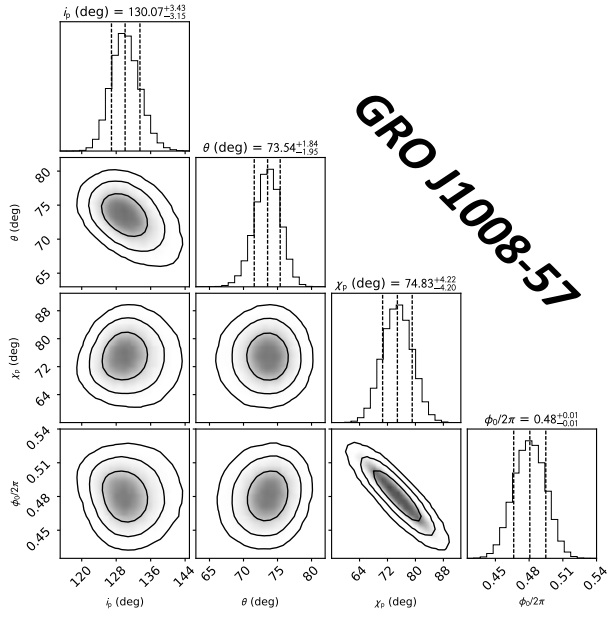

GRO J1008-57

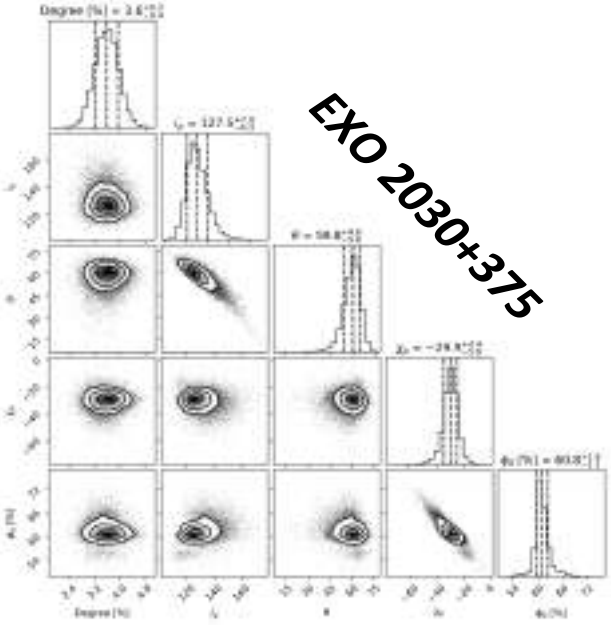

EXO 2030+375

Conclusions on polarimetry of XRPs

IXPE has opened a new window to the Universe. Observations of X-ray polarization are already revolutionizing our understanding of highly magnetized neutron stars. In the first two years of the observatory's operation, we:

- Demonstrated that the degree of polarization is lower than expected even in bright pulsars.
- For the majority of XRPs, we measured the geometry; for all of them, the inclinations of the orbit and the pulsar are in agreement; magnetic inclinations have a wide distribution.
- Discovered a non-pulsating polarized emission component in a pair of bright pulsars.
- Observed both correlation and anticorrelation of flux in the profile and degree of polarization.
- Confirmed the precession of the neutron star in Her X-1.

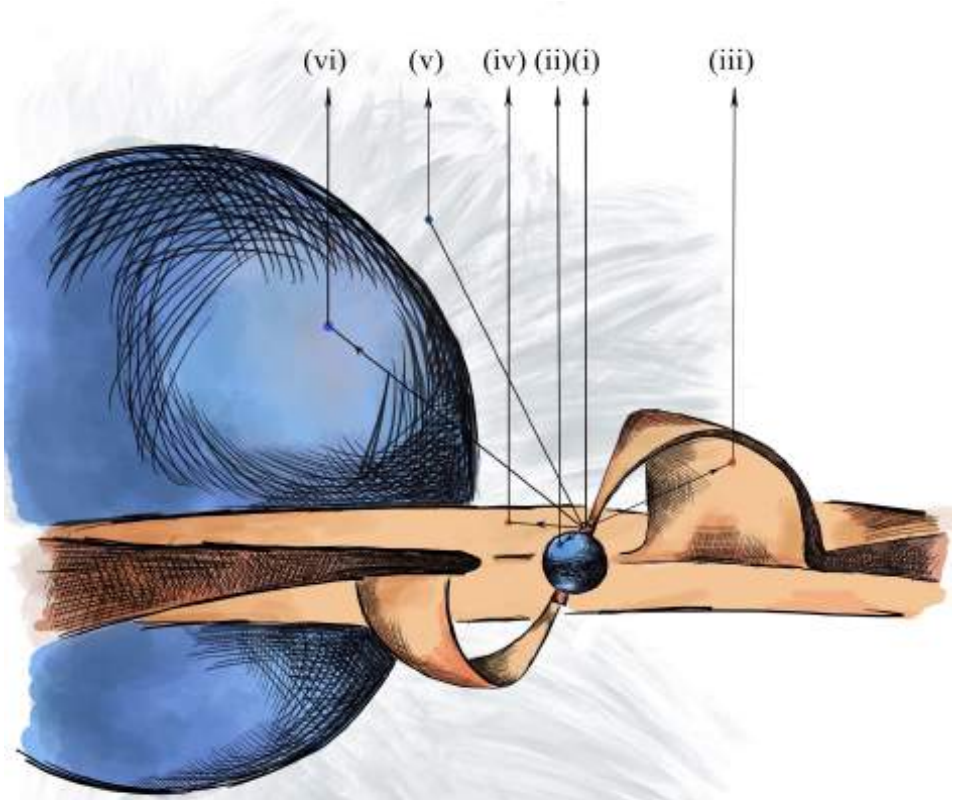

© Alexander Mushtukov